Dalton Transactions

Cite this: *Dalton Trans.*, 2011, **40**, 8377

www.rsc.org/dalton

PAPER

Valence and spin situations in isomeric $[(bpy)Ru(Q')_2]^n$ (Q′ = 3,5-di-*tert*-butyl-*N*-aryl-1,2-benzoquinonemonoimine). An experimental and DFT analysis†‡

Dipanwita Das,[a] Tapan Kumar Mondal,[b] Abhishek Dutta Chowdhury,[a] Fritz Weisser,[c] David Schweinfurth,[c] Biprajit Sarkar,[c] Shaikh M. Mobin,[a] Francisco A. Urbanos,§[d] Reyes Jiménez-Aparicio*[d] and Goutam Kumar Lahiri*[a]

Received 9th April 2011, Accepted 9th June 2011
DOI: 10.1039/c1dt10609k

The article deals with the ruthenium complexes, $[(bpy)Ru(Q')_2]$ (**1–3**) incorporating two unsymmetrical redox-noninnocent iminoquinone moieties [bpy = 2,2′-bipyridine; Q′ = 3,5-di-*tert*-butyl-*N*-aryl-1,2-benzoquinonemonoimine, aryl = C_6H_5 (Q'_1), **1**; *m*-$Cl_2C_6H_3$ (Q'_2), **2**; *m*-$(OCH_3)_2C_6H_3$ (Q'_3), **3**]. **1** and **3** have been preferentially stabilised in the *cc*-isomeric form while both the *ct*- and *cc*-isomeric forms of **2** are isolated [*ct*: *cis* and *trans* and *cc*: *cis* and *cis* with respect to the mutual orientations of O and N donors of two Q′]. The isomeric identities of **1–3** have been authenticated by their single-crystal X-ray structures. The collective consideration of crystallographic and DFT data along with other analytical events reveals that **1–3** exhibit the valence configuration of $[(bpy)Ru^{II}(Q'_{Sq})_2]$. The magnetization studies reveal a ferromagnetic response at 300 K and virtual diamagnetic behaviour at 2 K. DFT calculations on representative **2a** and **2b** predict that the excited triplet ($S = 1$) state is lying close to the singlet ($S = 0$) ground state with singlet–triplet separation of 0.038 eV and 0.075 eV, respectively. In corroboration with the paramagnetic features the complexes exhibit free radical EPR signals with g ~2 and ^{1}HNMR spectra with broad aromatic proton signals associated with the Q′ at 300 K. Experimental results in conjunction with the DFT (for representative **2a** and **2b**) reveal iminoquinone based preferential electron-transfer processes leaving the ruthenium(II) ion mostly as a redox insensitive entity: $[(bpy)Ru^{II}(Q'_Q)_2]^{2+}$ ($\mathbf{1}^{2+}$–$\mathbf{3}^{2+}$) ⇋ $[(bpy)Ru^{II}(Q'_{Sq})(Q'_Q)]^+$ ($\mathbf{1}^{+}$–$\mathbf{3}^{+}$) ⇋ $[(bpy)Ru^{II}(Q'_{Sq})_2]$ (**1–3**) ⇋ $[(bpy)Ru^{II}(Q'_{Sq})(Q'_{Cat})]^-$/$[(bpy)Ru^{III}(Q'_{Cat})_2]^-$ ($\mathbf{1}^{-}$–$\mathbf{3}^{-}$). The diamagnetic doubly oxidised state, $[(bpy)Ru^{II}(Q'_Q)_2]^{2+}$ in $\mathbf{1}^{2+}$–$\mathbf{3}^{2+}$ has been authenticated further by the crystal structure determination of the representative $[(bpy)Ru^{II}(Q'_3)_2](ClO_4)_2$ [**3**]$(ClO_4)_2$ as well as by its sharp ^{1}H NMR spectrum. The key electronic transitions in each redox state of $\mathbf{1}^n$–$\mathbf{3}^n$ have been assigned by TD–DFT calculations on representative **2a** and **2b**.

Introduction

Quinones, naturally occurring redox-active molecules, are involved in vital electron transport processes where they often interact with transition metal ions.[1] The quinone-containing prosthetic groups in metallo-quinoproteins,[2] pyrrolo-quinoline-quinone, tryptophan-tryptophyl-quinone, topaquinone, lysine-tyrosyl-quinone, vitamin K derivatives, ubiquinones or plasto-quinones play important roles as anti-oxidants (polyphenols), neurotransmitters (catecholamines), precursors of melanin pigments, energy conversion (photosynthesis, respiration) or information transfer agents.[3,4] This in turn has extended special impetus in designing metal–quinonoid based molecules as models for understanding the delicate valence, spin and electron-transfer aspects.[5,6] In this regard ruthenium–quinonoid(Q) frameworks have drawn continuous research interest primarily due to the unique feature of extensive delocalisation of dπ(Ru) and pπ(Q)

[a]*Department of Chemistry, Indian Institute of Technology Bombay, Powai, Mumbai, 400076, India. E-mail: lahiri@chem.iitb.ac.in*
[b]*Department of Chemistry, Jadavpur University, Jadavpur, Kolkata, 700032, India*
[c]*Institut für Anorganische Chemie, Universität Stuttgart, Pfaffenwaldring 55, D-70550, Stuttgart, Germany*
[d]*Departamento de Química Inorgánica, Facultad de Ciencias Químicas, Universidad Complutense, Ciudad Universitaria, E-28040, Madrid, Spain*

† Dedicated to Professor Wolfgang Kaim on the occasion of his 60th birthday.

‡ Electronic supplementary information (ESI) available: Crystallographic parameters, bond distances/angles, DFT data set, EPR and mass spectra (Figs. S1–S7 and Tables S1–S19). CCDC reference numbers 821453–821456. For ESI and crystallographic data in CIF or other electronic format see DOI: 10.1039/c1dt10609k

§ Deceased, May 28, 2011

based frontier orbitals.[7,8] This often introduces complexities in establishing the precise valence state configuration at the ruthenium–Q interface.[9] Moreover, the recently established application potential of ruthenium–quinonoid moieties in water oxidation processes has been an added attraction in dealing with such molecules.[10]

The easy accessibility of various oxidation states of ruthenium (+2, +3, +4) and quinonoid ligands (oxidised, Q_Q°; intermediate radical, $Q_{Sq}^{\bullet -}$; doubly reduced, Q_{Cat}^{2-}, Scheme 1) leads to the multiple electronic structure alternatives, $\{Ru^{II}–Q_Q\}\leftrightarrow\{Ru^{III}–Q_{Sq}\}\leftrightarrow\{Ru^{IV}–Q_{Cat}\}$.[11] The built in complexity may further be enhanced in a bis-quinonoid set up, $\{Ru–(Q)_2\}$ due to additional valence and spin-state interactions.[11]

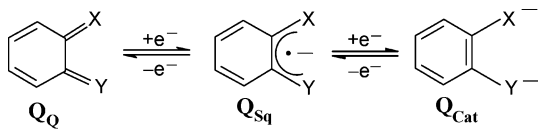

Scheme 1

The extent of delocalisation of frontier orbitals of Ru and Q is known to vary significantly depending on the specific electronic nature of the quinonoid moieties (Scheme 1) as well as the associated ancillary ligands (AL) in the complexes.[7–9] In this context a wide variety of quinonoid frameworks (Scheme 1) along with ruthenium precursors involving different ancillary ligands such as 2,2′-bipyridine (bpy),[7l,m,n,v] 2,2′:6′,2″-terpyridine (trpy),[9b,k,o] 2-phenylazopyridine (pap),[9g,n] acetylacetonate (acac),[7i,8g,9c,12c] PPh_3,[13c,d,14] NH_3,[7s,x,8h] CO,[13e] NO,[9k] Cl^-[14] have been scrutinised at the mononuclear level. The earlier studies are mostly restricted to the single quinonoid ligand coordinated to the octahedrally surrounded metal ion in {(AL)Ru–Q} and in a few cases the *tris*-complexes, $\{Ru–(Q)_3\}$ have also been examined.[12] To the best of our knowledge the following few examples related to the intermediate situation of two quinonoid ligands around the ruthenium ion are known so far. The diamagnetic $S = 0$ ground state in $\{(AL)Ru^{II}(Q_{Sq})_2\}$: Q = X = Y = O (Scheme 1), AL = bpy,[13a] ^{t}Bu-Py,[13b] PPh_3,[13c,d] CO[13e] or Q = X = Y = NH, AL = bpy[13f] has been reported to develop *via* the strong antiferromagnetic coupling of two radical Q_{Sq} ligands or selective stabilisation of the fully-oxidised diiminoquinone state (Q_Q), respectively. The three-spin situation in $[(acac)Ru^{III}((Q'_1)_{Sq})_2]$ yields a doublet ($S = 1/2$) ground state *via* the antiferromagnetic coupling between the unpaired spins on Ru^{III} and one of the Q_{Sq} centres.[12c]

Considering the inherent sensitivity of valence and spin distribution processes in the {Ru–Q} set up, the present work is specifically aimed at investigating the interactions of two unsymmetrical iminoquinones (Q′ = X = O, Y = NPhR, Scheme 1) with the ruthenium centre in $[(bpy)Ru(Q')_2]$. This specific choice of Q′ as the quinonoid framework for the present study primarily originated from our recent observations that the ruthenium coordinated Q′ can exhibit substantial variations with respect to the analogous iminoquinone, Q = X = O, Y = NH or dioxolene, Q = X = Y = O (Scheme 1) particularly towards the Ru–Q based electron-transfer processes.[9c,g,n,12c,13c] Moreover, unlike the recently reviewed[15] well developed chemistry of first row transition metal ions of Q′, the corresponding ruthenium chemistry is confined to a limited number of recent reports.[8o,9g,12c]

The present article describes the detailed synthetic and structural aspects of the bis-iminoquinone complexes in the framework of $[(bpy)Ru(Q')_2]$ (**1–3**) including their isomeric structural features. The delicate intramolecular valence and spin-state aspects in accessible redox-states of $\mathbf{1}^n$–$\mathbf{3}^n$ ($n = +2, +, 0, –$) have been addressed by experimental and DFT results as well as in relation to the reported analogous systems.[13]

Results and discussion

Synthesis and isomeric features

The complexes $[Ru(bpy)(Q')_2]$, **1–3** have been synthesized from $Ru^{III}(bpy)Cl_3$ (bpy = 2,2′-bipyridine) and the respective ligands, $H_2Q'_{1-3}$ (Scheme 2 and see the Experimental section) in the presence of NaOH as a base.

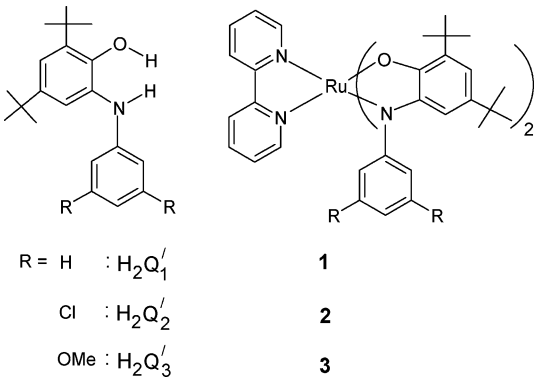

Scheme 2

The presence of two unsymmetrical ligands (Q′) in **1–3** introduces the possibility of three geometrical isomeric forms, *cc*(all *cis*), *ct*(*N-trans*) and *tc*(*O-trans*) with respect to the oxygen and nitrogen donors of the two Q′ (Scheme 3). Though **1** (Fig. S1 in the Supplementary information‡) and **3** (Fig. 2) have been found to stabilise selectively in the *cc*-isomeric form, the *ct*-and *cc*-isomeric forms of complex **2** have been isolated as major (**2a**) and minor (**2b**) products (Fig. 1), respectively.

Unlike **1** and **2**, complex **3** with OMe substituents in the 3- and 5- positions of the pendant phenyl ring of Q'_3 (Scheme 2) partially transforms to the corresponding doubly oxidised state, $\mathbf{3}^{2+}$ during the purification step using a silica gel column. Therefore, both **3** and doubly oxidised $\mathbf{3}^{2+}$ (in the form of $[\mathbf{3}](ClO_4)_2$) have been eluted from the same column by CH_3CN and CH_3OH–$HClO_4$ mixture, respectively, and subsequently structurally characterised (see the Experimental section).

The electrically neutral **1–3** exhibit satisfactory microanalytical and mass spectral data in CH_3CN (see the Experimental section and Fig. S2‡).

Structural aspects

The single crystal X-ray structures of **2a**, **2b** and **3** are shown in Fig. 1 and 2, respectively. The selected crystallographic parameters, bond distances and angles are listed in Table 1, Table 2 and

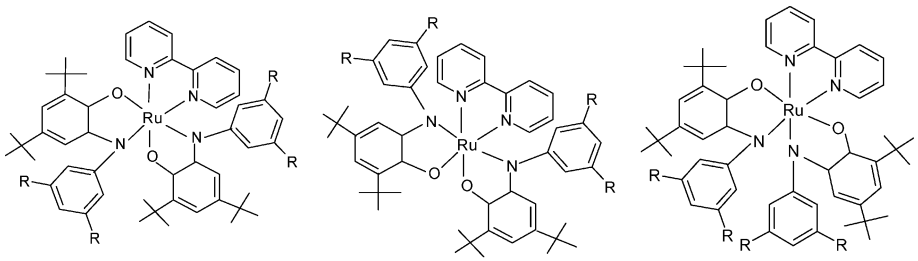

cc(all *cis*) ***ct***(N-*trans*) ***tc***(O-*trans*)

Scheme 3

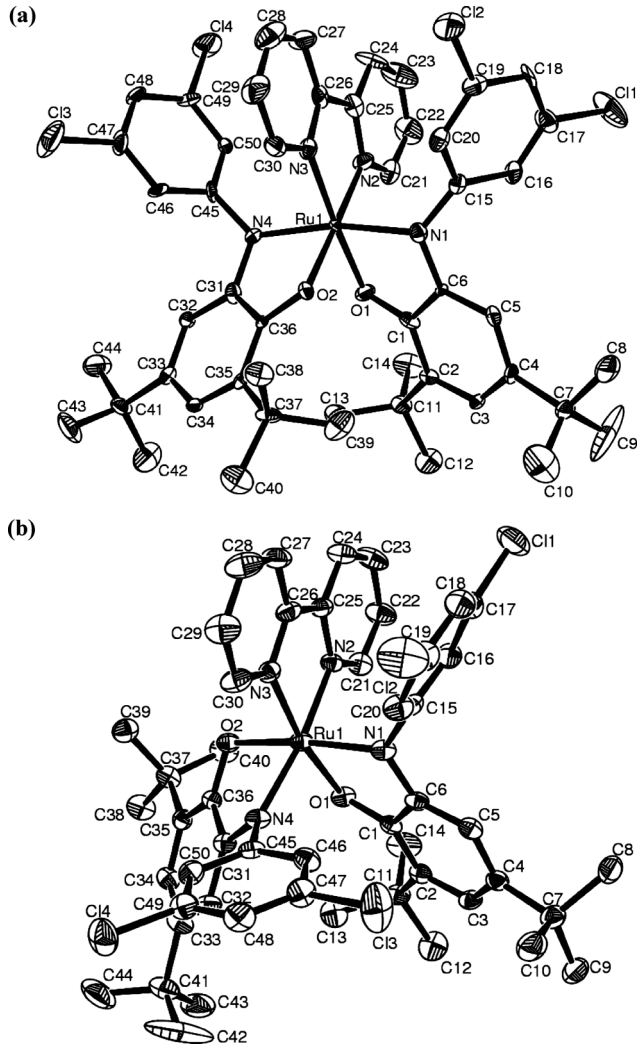

Fig. 1 ORTEP diagrams of (a) **2a** and (b) **2b**. Ellipsoids are drawn at 50% probability. Hydrogen atoms are omitted for clarity.

Table S3,‡ respectively. It should be noted that in spite of several attempts the refinement of the reasonably good quality data set for the crystal of **1** always led to a higher "R" factor (Fig. S1 and Tables S1, S2‡), presumably due to some sort of intrinsic crystallographic problems. However, it always crystallises in the *cc*-geometric form and the relevant bond distances are close to other structurally well characterised derivatives, **2a**, **2b** and **3** (see below).

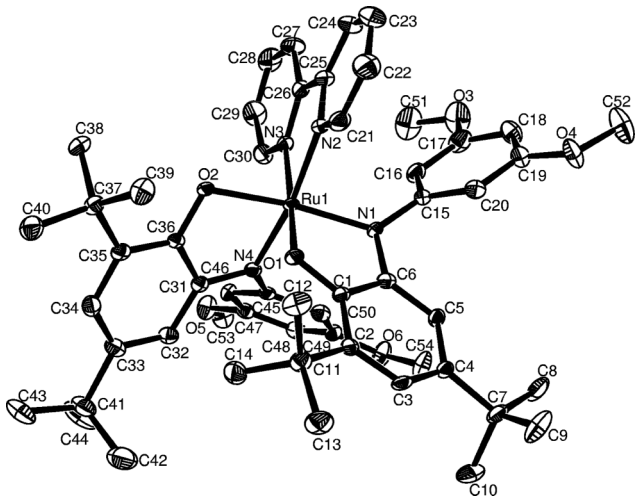

Fig. 2 ORTEP diagram of **3**. Ellipsoids are drawn at 50% probability. Hydrogen atoms are omitted for clarity.

The sensitive[9a,c,14] C–O, C–N and intra-ring bond distances associated with the coordinated Q′ in **1–3** (Table 2 and Table S2‡) reveal the following important features: (i) Both the iminoquinonoid moieties (Q′) exist in the same redox state leading to the valence formalism of either $[Ru^{II}(bpy)(Q'_{Sq})_2]$ or $[Ru^{IV}(bpy)(Q'_{Cat})_2]$. (ii) The C–O and C–N bond distances of the coordinated Q′ in **1–3** exhibit a rather complex relationship where the C–O distances are somewhat closer to the localised Q'_{Sq} distance of 1.30 Å whereas C–N distances correspond to the localised Q'_{Cat} form of 1.38 Å.[9a,c,14] As a consequence the C–C(*meta*) distances of the coordinated Q′ appear to be slightly longer than the ideal C–C(*meta*) distance of 1.36 Å for the Q'_{Sq} state.[9a,c,14] However, the shorter C–C(*meta*) distances relative to the other intra-ring distances in each case signifies the presence of Q'_{Sq} state in **1–3** leading to the overall composition of $[(bpy)Ru^{II}(Q'_{Sq})_2]$. The elongation of C–O, C–N and intra-ring C–C(*meta*) bond distances of Q′ in **1–3** (Table 2 and Table S2‡) with respect to the localised Q'_{Sq} distances[14] can be attributed to the effect of delocalisation of Ru and Q'_{Sq} based frontier orbitals.[9a,b,o] The delocalisation of metal-quinonoid based orbitals in redox active transition metal complexes and its subsequent consequence on the electronic structures has been addressed in detail by Wieghardt *et al.*[6] Moreover, the superposition of resonating states in ruthenium–quinonoid systems may also yield the intermediate description as stated by Remenyi and Kaupp.[9a]

Table 1 Selected crystallographic data for **2a**, **2b**, **3** and **[3]**$(ClO_4)_2$

	2a	**2b**	**3**	**[3]**$(ClO_4)_2$
Empirical formula	$C_{50}H_{54}Cl_4N_4O_2Ru$	$C_{50}H_{54}Cl_4N_4O_2Ru$	$C_{54}H_{66}N_4O_6Ru$	$C_{54}H_{66}Cl_2N_4O_{14}Ru$
M_r	985.84	985.84	968.18	1167.08
Crystal symmetry	Triclinic	Monoclinic	Triclinic	Monoclinic
Space group	$P\bar{1}$	$P2_1/n$	$P\bar{1}$	$P2_1/c$
a/Å	8.8394(4)	11.6914(4)	10.1872(3)	24.2408(3)
b/Å	12.3326(5)	17.2733(4)	15.1077(5)	11.46730(10)
c/Å	23.5067(10)	23.6512(7)	17.2960(4)	20.0408(2)
α (°)	103.280(4)	90	78.698(2)	90
β (°)	96.488(4)	101.160(3)	82.659(2)	92.3590(10)
γ (°)	100.985(4)	90	71.615(3)	90
V/Å^3	2415.13(18)	4686.0(2)	2470.86(12)	5566.15(10)
Z	2	4	2	4
μ/mm^{-1}	0.588	0.606	0.370	0.445
T/K	150(2)	150(2)	150(2)	150(2)
D_c/g cm^{-3}	1.356	1.397	1.301	1.393
F(000)	1020	2040	1020	2432
2θ range (deg)	3.21 to 25.00	3.25 to 25.00	3.30 to 25.00	3.31 to 25.00
Data, restraints, parameters	8498/81/562	8230/0/562	8681/0/602	9789/0/692
Final R_1, wR_2 [$I > 2\sigma(I)$]	0.0677, 0.0589	0.0338, 0.0607	0.0468, 0.1119	0.0399, 0.0931
R_1, wR_2 (all data)	0.1622, 0.0734	0.0618, 0.0638	0.0586, 0.1157	0.0602, 0.0972
GOF	0.776	0.817	0.998	0.916
largest diff. peak/hole/e Å^{-3}	0.755 and –0.760	0.407 and –0.387	1.939 and –0.846	0.994 and –0.646

Table 2 Selected bond distances (Å) in **2a**, **2b**, **3** and $\mathbf{3}^{2+}$

	2a		**2b**		**3**	$\mathbf{3}^{2+}$
Bond distances	X-Ray	DFT	X-Ray	DFT	X-Ray	X-Ray
Ru(1)–O(1)	2.003(4)	2.049	2.012(2)	2.040	2.007(2)	2.049(2)
Ru(1)–N(1)	1.980(5)	2.046	1.960(2)	2.039	1.991(3)	1.990(2)
Ru(1)–N(2)	2.037(5)	2.059	2.057(2)	2.081	2.073(2)	2.045(2)
Ru(1)–N(4)	1.995(5)	2.045	2.001(2)	2.043	1.996(2)	2.021(2)
Ru(1)–N(3)	2.032(5)	2.059	2.060(2)	2.080	2.077(3)	2.033(3)
Ru(1)–O(2)	2.025(4)	2.050	2.023(2)	2.048	2.020(2)	2.023(2)
C(1)–O(1)	1.320(6)	1.323	1.318(3)	1.325	1.317(4)	1.272(3)
C(6)–N(1)	1.382(6)	1.378	1.384(3)	1.389	1.397(4)	1.321(4)
C(36)–O(2)	1.312(6)	1.324	1.331(3)	1.322	1.335(3)	1.270(3)
C(31)–N(4)	1.407(7)	1.379	1.391(3)	1.387	1.381(4)	1.327(4)
C(2)–C(3)	1.393(7)	1.389	1.376(4)	1.386	1.384(5)	1.362(4)
C(4)–C(5)	1.375(7)	1.382	1.374(4)	1.390	1.377(4)	1.343(4)
C(32)–C(33)	1.375(8)	1.382	1.366(4)	1.382	1.371(5)	1.345(4)
C(34)–C(35)	1.385(8)	1.390	1.380(4)	1.385	1.389(4)	1.370(4)

Table 3 Spin densities of complexes calculated from DFT[a]

Complexes	Q′	Ru	bpy
2a[b]	1.731	0.312	–0.043
2a^{+}[c]	1.273	–0.280	0.007
2a^{-}[c]	0.707	0.436	–0.143
2b[b]	1.698	0.326	–0.024
2b^{+}[c]	1.127	–0.126	–0.0008
2b^{-}[c]	0.608	0.411	–0.019

[a] From (U)B3LYP calculations. [b] Triplet state. [c] Doublet state.

The complexes exhibit free radical EPR signals with $g \sim 2.0$ at 300 K (Fig. S3‡) (see later). The DFT calculated bond parameters based on the optimised isomeric **2a** and **2b** in triplet state (Fig. S4‡) match fairly well with the experimental data (Table 2 and Table S3‡). The spin density plots of **2a** and **2b** (Fig. 3a, 3b, Table 3) reveal that the Q'_{Sq} moieties are the primary spin bearing centres with partial delocalisation onto the metal site. The natural bond orbital analysis (NBO) predicts an electronic configuration of Ru(4d) of 6.93 and 6.88 in **2a** and **2b**, respectively, (Tables S4, S5‡) which also collectively favours the valence formulation of $[(bpy)Ru^{II}(Q'_{Sq})_2]$. In agreement with a $\{Ru^{II}–(Q'_{Sq})_2\}$ configuration, **1–3** exhibit intense low-energy transition near 1000 nm (see later).[9g] It should be noted that the slight metal contribution in the spin-density plots (Table 3, Fig. 3a, 3b) as well as in the SOMOs (SOMO = singly occupied molecular orbital) of **2a** and **2b** as predicted by DFT (Table S6a and Table S7‡) has also been partly resolved in the slightly structured EPR spectra (Fig. S3‡) under the experimental conditions. This implies the minor existence of the alternate resonance form of $\{(bpy)Ru^{III}(Q'_{Sq})(Q'_{Cat})\}$.[16]

The valence configurations of the reported diamagnetic bis-quinonoid complexes, $[(bpy)Ru(Q)_2]$[13a] and *trans*-$[(^tBu\text{-}Py)_2Ru(Q)_2]$[13b] (Q = X = Y = O, Scheme 1), have been defined as $\{(bpy)Ru^{II}(Q_{Sq})_2\}\leftrightarrow\{(bpy)Ru^{III}((Q_{Cat})(Q_{Sq})\}$ and $\{(^tBu\text{-}Py)_2Ru^{II}(Q_{Sq})_2\}\leftrightarrow\{(^tBu\text{-}Py)_2Ru^{IV}(Q_{Cat})_2$, respectively, primarily based on the intermediate C–O bond distances (average) of 1.321(5) Å (Table 4). On the other hand, the average C–O distances of 1.309(5), 1.296(10) and 1.301(11) Å in

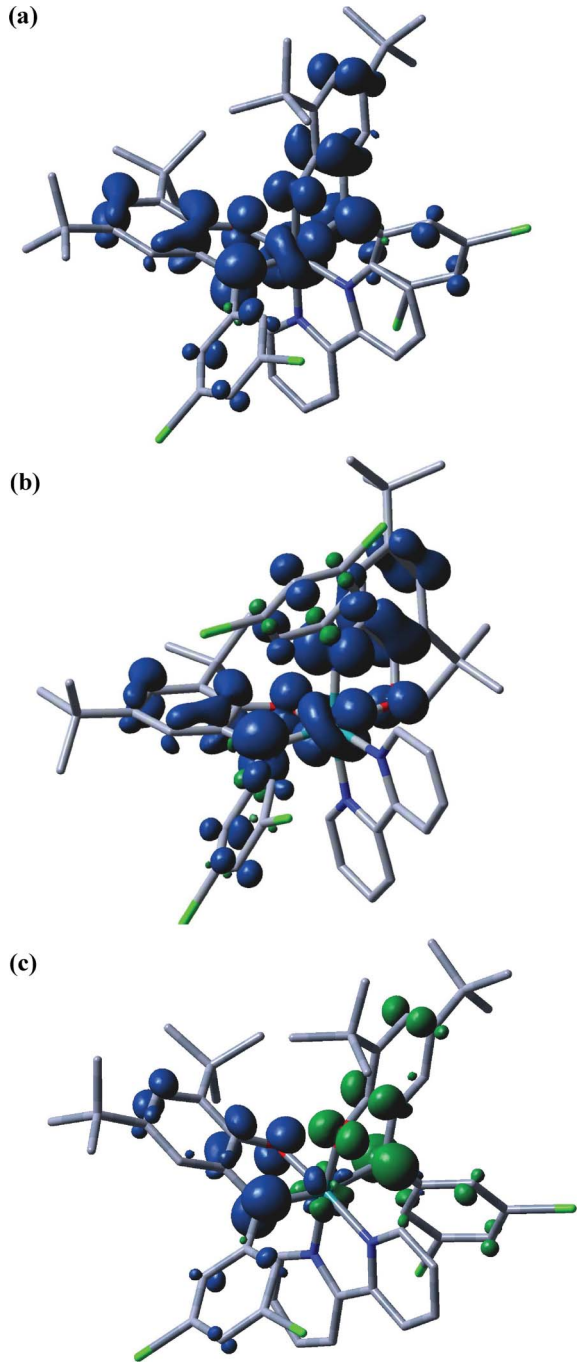

Fig. 3 DFT calculated spin density plots of (a) **2a**, (b) **2b** and (c) **2a** (BS(1,1)).

diamagnetic *trans*-[$(PPh_3)_2Ru^{II}(Q)_2$], *cis*-[$(PPh_3)_2Ru^{II}(Q)_2$][13c,d] and *cis*-[$(CO)_2Ru^{II}(Q)_2$],[13e] respectively, (Table 4) match fairly well with the localised Q_{Sq} state.

Magnetic properties

The magnetic properties of representative **1** and **2a** have been explored, which display similar room temperature magnetic behaviour. In both cases the magnetization measurements towards the magnetic field at 300 K show a rapid increase in magnetization at very low magnetic fields to reach close to the constant values corresponding to $S = 0.07$, and $S = 0.01$, respectively (Fig. 4a and S5a‡). On the other hand, at 2 K, the magnetization measurements towards the magnetic field show lower values than those expected from the Brillouin formula for a system with two $S = 1/2$ spins (Fig. 4b and S5b‡). These measurements indicate the existence of an almost antiferromagnetic behaviour particularly at low temperature. However, the shape of the magnetization curves at 300 K and also the values obtained (Fig. 4 and S5‡) are attributed to the presence of unpaired electrons primarily located on the two iminosemiquinone moieties Q′ in **1** and **2a** as revealed by the radical EPR spectra (Fig. S3‡) as well as up-field shifted broad proton resonances involving the Q′ (Fig. 5, see later).

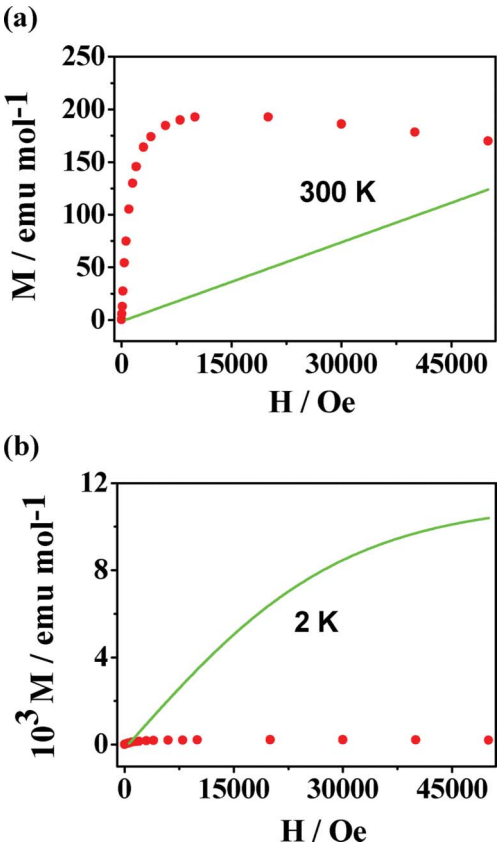

Fig. 4 Representation of the magnetization towards magnetic field from 0 to 5 T of **2a** measured at (a) 300 K and (b) 2 K. Solid line represents the calculated curve for a system with two $S = 1/2$ spins.

The non-linearity of the magnetization curves and the fast increase of the magnetization values at 300 K at very low magnetic fields indicate the existence of a ferromagnetic state which is in accordance with magnetization values higher than that predicted by the Brillouin equation. The virtual antiferromagnetic behaviour at low temperature and ferromagnetic response at higher temperature can be interpreted in terms of the existence of a singlet ground state with a thermally accessible low-lying excited $S = 1$ state[6c,17] as is evidenced by the DFT calculations on **2a** where the triplet ($S = 1$) state is 0.038 eV above the singlet ($S = 0$) ground state. However, the non-linearity of the magnetization curve towards the magnetic field has prevented us from calculating the susceptibility values and therefore from simulating the experimental data. The said magnetic behaviour at

Table 4 C–O distances of coordinated Q in reported $\{Ru(Q)_2\}$species (Q: X = Y = O, Scheme 1)

Complexes	C–O bond distances(Å)	C–O bond distances (Avg.)(Å)	Spin state	Ref.
$Ru(bpy)(C_6H_4O_2)_2$	1.316(5) 1.326(6) 1.322(4) 1.321(5)	1.321(5)	$S = 0$	13a
trans-$Ru(4\text{-t-Bupy})_2(3,5\text{-}^tBuC_6H_2O_2)_2$	1.320(5) 1.322(5)	1.321(5)	$S = 0$	13b
trans-$Ru(PPh_3)_2(Cl_4C_6O_2)_2$	1.307(4) 1.312(5)	1.309(5)	$S = 0$	13c
cis-$Ru(PPh_3)_2(Cl_4C_6O_2)_2$	1.296(8) 1.289(9) 1.287(10) 1.312(12)	1.296(10)	$S = 0$	13d
cis-$Ru(CO)_2(3,6\text{-}^tBuC_6H_2O_2)_2$	1.284(11) 1.302(10) 1.324(12) 1.295(13)	1.301(11)	$S = 0$	13e

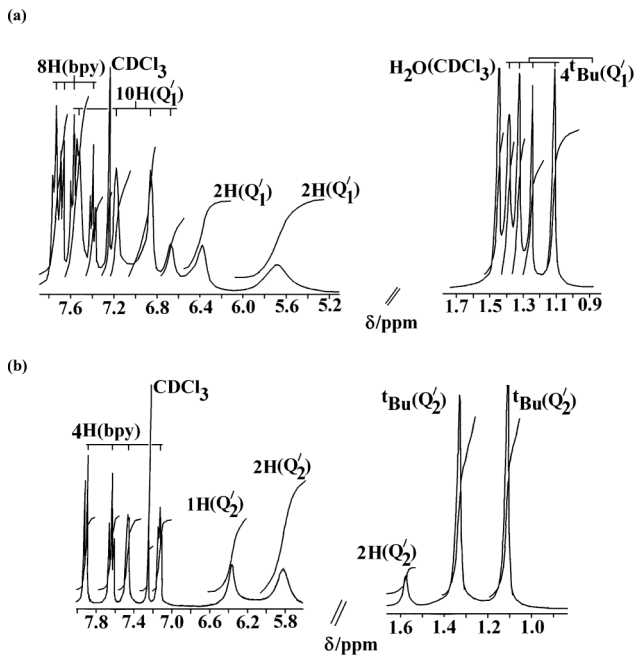

Fig. 5 ^{1}H NMR spectra of (a) **1** and (b) **2a** in $CDCl_3$.

room-temperature could be tentatively attributed to the magnetic anisotropic feature of the complexes under the applied magnetic field.[18]

The complexes exhibit EPR signals with g ~2.00, at 300 K (Fig. S3‡). However, the complexes are EPR inactive at 4 K in accordance with their virtual diamagnetic nature near 2 K as revealed by the magnetic studies. The line widths of the EPR signals are consistent with a ligand radical assignment. The absence of significant g anisotropy implies the negligible participation of the metal ion as also indicated by the spin density plots (Table 3, Fig. 3a, 3b). The expected half-field signal for the diradical has not been resolved at the experimental conditions (X-band, 300 K). The observed $S = 1/2$ type EPR signal and the absence of a half-field feature suggest a diradical with weakly interacting iminosemiquinone spins (see below).[19] A look at the SOMOs confirms that the spin-bearing π orbitals of the iminosemiquinone moieties are neither parallel nor anti-parallel but are almost perpendicular to each other (~70° on optimised geometry, Fig. 6 and Tables S6a, S7‡).

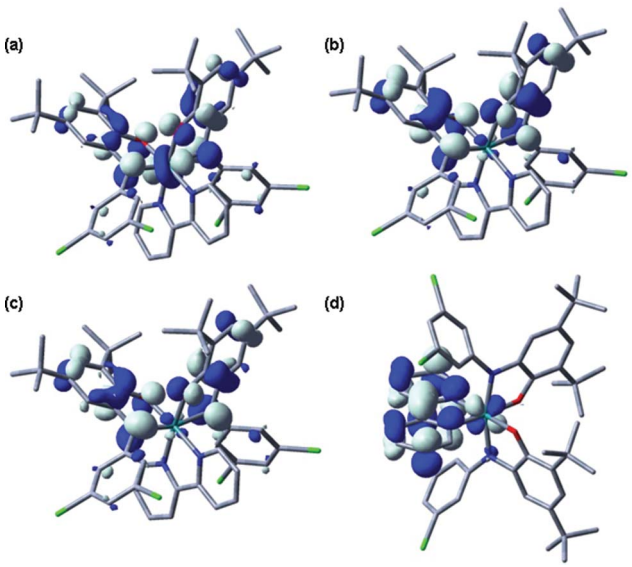

Fig. 6 Representative orbital contour diagrams of **2a** (S = 1 state), (a) SOMO1(α-spin), (b) SOMO2(α-spin), (c) LUMO(β-spin) and (d) LUMO+1(β-spin).

To understand the electronic features further, three possible spin situations of **2a** were taken into consideration: (i) a simple closed shell spin restricted model, (ii) an open shell BS(1,1) (broken symmetry) model[6h,20a,21] corresponding to two ligand radicals coupled antiferromagnetically *via* the super exchange pathway mediated by one of the t_{2g} orbitals of a low-spin d^6-ruthenium ion and (iii) an open shell triplet model. The energy of the BS(1,1) state is found to be lower with respect to the corresponding closed shell solution by 0.112 eV at the B3LYP level of theory. This has also been verified using other density functionals with different functional exchange where the energy differences between BS(1,1) and closed shell singlet are calculated to be 0.093 eV and 0.106 eV at TPSS and BMK levels, respectively, implying the singlet diradical situation.[20] In the open shell BS(1,1) model at

the B3LYP level of theory, two ligand centred SOMOs (**X**, **Y**, see below) of opposite spin are identified (Table S6b‡).

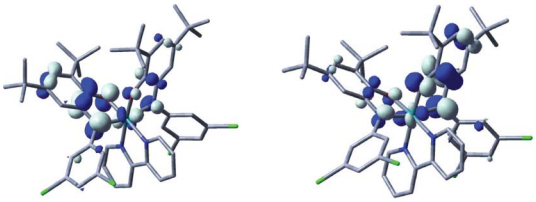

SOMO(α-spin) (**X**) SOMO(β-spin) (**Y**)

The antiferromagnetic coupling between these two orbitals *via* any of the metal t_{2g} orbitals gives rise to a relatively moderate mutual spatial overlap (S_{ab}) of 0.58 indicating weakly antiferromagnetically coupled biradical character within the molecule (see Experimental section for details). It should be noted that antiferromagnetism is a function of the mutual spatial overlap (S_{ab}), in a closed shell it becomes unity and in the non-interacting case it becomes zero.[6h,20a] The spin density population (BS(1,1)) analysis (Fig. 3c) again exhibits the anti-parallel spin alignment of two radical ligands. The diradical character in the present case can be rationalised on the basis of a specific alignment of spins which may be due to the observed ferromagnetic behaviour at room-temperature.

It should be noted that the ruthenium-bis-quinonoid complexes of the general formula of $[(PR_3)_2Ru^{II}(Q_{Sq})_2]$ (Q = X = Y = O, Scheme 1) have been recently established to exhibit a weak temperature, ligand and solvent dependent residual paramagnetism in spite of the fact that the complexes do not have any detectable magnetic moment. This has been addressed in terms of singlet–triplet equilibria where the low-lying triplet ($S = 1$) state exists 0.132–0.170 eV (depending on the nature of R groups of PR_3) above the singlet ($S = 0$) ground state.[22]

1–3 exhibit ^{1}H NMR spectra with broad aromatic signals associated with the quinonoid moieties.[9d,e,j,22,23] However, proton resonances due to the bpy ligand in the complexes appear as normal doublets and triplets in the expected region of δ 8.50–7.50 ppm[24] (Fig. 5). The *ct*(*N-trans*) isomer **2a** exhibits 4 and 5 aromatic proton signals of bpy and Q'_2, respectively, corresponding to half of the molecule while the *cc*-isomeric forms **1**, **2b** and **3** show aromatic protons due to the full molecule. Accordingly, **1**, **2b**, **3** and **2a** exhibit four and two ^{t}Bu signals in the up-field region, respectively. The OMe-resonances in **3** appear as two singlets at δ, 3.60 and 3.27 ppm.

Redox and spectroelectrochemical aspects

1–3 exhibit three similar redox steps: two successive one-electron oxidation processes and one reduction within the potential window of ± 2.0 V *versus* SCE in CH_3CN (Fig. 7 and Table 5). In the *cc*-isomeric framework of **1**, **2b** and **3** (Scheme 3) the potentials are found to vary depending on the electronic nature of the "R" groups[9g,25] present in the quinonoid ligands, Q'_{1-3} (Scheme 2) and the redox potentials follow the order: **2b**(Cl) > **1**(H) > **3**(OMe). Between the *ct*-isomeric **2a** and the *cc*-isomeric **2b** the first oxidation and reduction potentials of the former are lower than those of the latter. The comproportionation constant (K_c)[26] values of 10^{7-10} for the two successive oxidation processes (ox I and ox II) are much lower than those of 10^{15-19} calculated on the basis of the first oxidation and first reduction processes (ox I and red I)

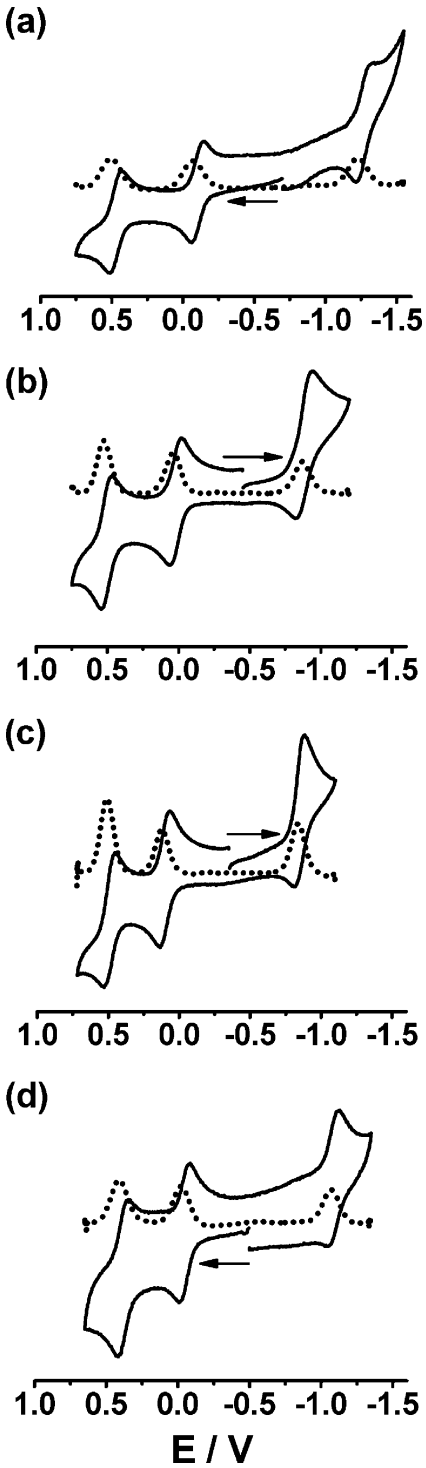

Fig. 7 Cyclic voltammograms (—) and differential pulse voltammograms (---) of (a) **1**, (b) **2a**, (c) **2b** and (d) **3** *versus* SCE in CH_3CN, 0.1 mol dm^{-3} Et_4NClO_4. Scan rate 100 mV s^{-1}.

(Table 5) which implies the redox-stability of the isolated form of $[(bpy)Ru(Q'_{Sq})_2]$ in **1–3**. The more basic iminoquinone form (Q′) in **1–3** as compared to the dioxolene form in [Ru(bpy)(3,5-^{t}Bu-$C_6H_4O_2)_2$][13a] makes the oxidation processes relatively easier and reduction process relatively difficult in **1–3**.[9i] As a consequence, the expected reduction of the second Q'_{Sq} as well as reductions

Table 5 Redox potentials and comproportation constants for **1–3** and Ru(bpy)(3,5-^{t}Bu-$C_6H_4O_2$)$_2$

	E°_{298}/V (ΔE_p/mV)						
Complexes	ox II	ox I	red I	red II	K_{c1}[c]	K_{c2}[c]	K_{c3}[c]
1[a]	0.47(70)	–0.10(80)	–1.25(100)	—	$10^{9.6}$	$10^{19.4}$	—
2a[a]	0.50(90)	0.02(50)	–0.87(100)	—	$10^{8.1}$	$10^{15.0}$	—
2b[a]	0.50(90)	0.10(80)	–0.83(70)	—	$10^{6.7}$	$10^{15.7}$	—
3[a]	0.38(70)	–0.05(70)	–1.09(70)	—	$10^{7.2}$	$10^{17.6}$	—
Ru(bpy)(3,5-^{t}Bu-$C_6H_4O_2$)$_2$[b]	0.89	0.20	–0.82	–1.53	$10^{10.8}$	$10^{15.2}$	$10^{13.8}$

[a] In CH_3CN–0.1 mol dm^{-3} Et_4NClO_4, *versus* SCE, scan rate 100 mV s^{-1}. [b] In 1,2-dichloroethane–0.1 mol dm^{-3} Et_4NClO_4, *versus* SCE, scan rate 200 mV s^{-1}. [c] $RT\ln K_c = nF(\Delta E)$ for T = 298 K. K_{c1}, K_{c2}, K_{c3} correspond to successive two oxidation processes, first oxidation and reduction processes, the first and second reduction processes in Ru(bpy)(3,5-^{t}Bu-$C_6H_4O_2$)$_2$, respectively.

Table 6 Electronic spectral data of [**1**]^n–[**3**]^n in CH_3CN

Compound	λ_{max}/nm (ε/dm^3 mol^{-1}cm^{-1})
1^{2+}	646(11600), 465(3940)
1$^+$	953(1940), 664(7410), 482(7040)
1	954(12580), 540(8980), 358(9210), 293(21690)
2a^{2+}	660(8600), 492(4180)
2a$^+$	968(1750), 677(9030), 488(7730)
2a	972(14030), 547(9130), 338(12650), 293(23980)
2a$^-$	912(8620), 633(6110), 472(7240), 341(20140)
2b^{2+}	658(8620), 488(4040)
2b$^+$	970(1750), 678(9040), 490(7730)
2b	993(9440), 554(8750), 359(10280), 293(23290)
2b$^-$	912(6610), 641(5740), 477(6240), 363(15010)
3^{2+}	648(8370), 462(3320)
3$^+$	958(1580), 671(13200), 463(8510)
3	962(14950), 542(10970), 362(11660), 291(25050)

of the coordinated bpy ligand[13a] in **1–3** have moved beyond the experimental potential limit of –2.0 V *versus* SCE.

The molecular orbitals obtained by open-shell triplet state (S = 1) calculations on **2a** and **2b** are summarised in Tables S6a and S7,‡ respectively. The singly occupied molecular orbitals of α-spin (SOMO1 and SOMO2) in the complexes have a major contribution from the in- and out-of-phase combinations of the lowest π* orbitals of two Q′ ligands with partial contribution from Ru non-bonding d-orbitals (Fig. 6). The other low-lying occupied MOs have both Ru(dπ) and Q′ character. The LUMO of β-spin corresponds to SOMO2 of α-spin has ~95% Q′ character while LUMO+1 (β-spin) corresponding to LUMO of α-spin has 85–93% bpy contribution.

The SOMO1 and SOMO2 in each case are composed of ~75% and ~95% Q′ based orbitals, respectively, (Tables S6a and S7‡). Similarly, SOMO in the doublet state (S = 1/2) of the first oxidised **2a**$^+$ or **2b**$^+$ is also dominated by the Q′ based orbitals (~95%) (Tables S8, S9‡). This in effect implies the quinone based preferential successive oxidation processes, ox-I and ox-II (Fig. 7, Table 5) leaving the ruthenium(II) ion as a redox insensitive entity: [(bpy)Ru^{II}(Q′$_{Sq}$)$_2$] (**1–3**) → [(bpy)Ru^{II}(Q′$_{Sq}$)(Q′$_Q$)]$^+$ (**1**$^+$–**3**$^+$) → [(bpy)Ru^{II}(Q′$_Q$)$_2$]$^{2+}$ (**1**$^{2+}$–**3**$^{2+}$). In agreement with the [(bpy)Ru^{II}(Q′$_{Sq}$)(Q′$_Q$)]$^+$ configuration of the first oxidised state instead of the alternate [(bpy)Ru^{III}(Q′$_{Sq}$)$_2$]$^+$, **1**$^+$–**3**$^+$ exhibit the following: (i) Free radical EPR spectra with g ~ 2.0 (Fig. S6‡) corresponding to the presence of unpaired spin selectively on the Q′$_{Sq}$ centre (Fig. 8, Table 3). (ii) A low-energy transition near 950 nm characteristic of the {Ru^{II}–Q′$_{Sq}$} configuration (Table 6, Fig. 12).[9g,12c,27] (iii) The DFT calculated C–O and C–N bond distances of coordinated Q′$_2$ are, as expected, in the decreasing mode on moving from **2**→**2**$^+$ (Tables S14, S15‡). (iv) An appreciable mixing of ruthenium(II) and Q′ based orbitals in the LUMO (α-spin, ~40% Ru and ~60% Q′, Tables S8, S9‡) of **2a**$^+$ or **2b**$^+$ due to a (dπ)Ru^{II}→(π*)Q′ back-bonding interaction.[7i]

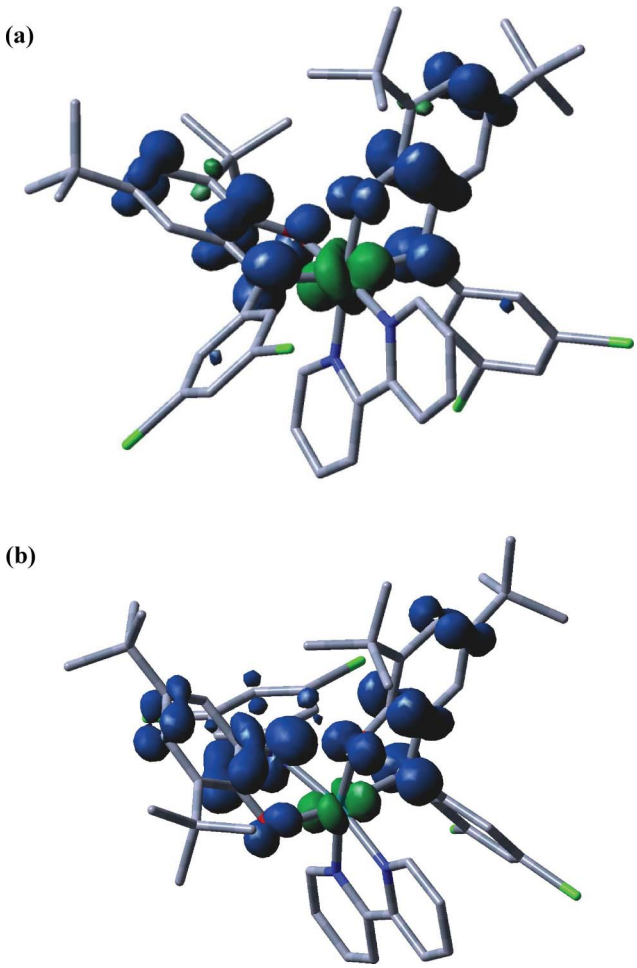

Fig. 8 DFT calculated spin density plots of (a) **2a**$^+$ and (b) **2b**$^+$.

The valence configuration of the EPR inactive doubly oxidised state of [(bpy)Ru^{II}(Q′$_Q$)$_2$]$^{2+}$ in [**1–3**]$^{2+}$ (Tables S10 and S11‡) has been authenticated *via* the crystal structure determination of the isolated [(bpy)Ru^{II}(Q′$_3$)$_2$](ClO$_4$)$_2$, [**3**](ClO$_4$)$_2$ (Fig. 9, Tables 1 and 2).[5h,r,7a,9m] The average distances of C–O, C–N and C–C(intra ring) bonds of the coordinated Q′$_3$ in **3**$^{2+}$ of 1.271(3), 1.324(4),

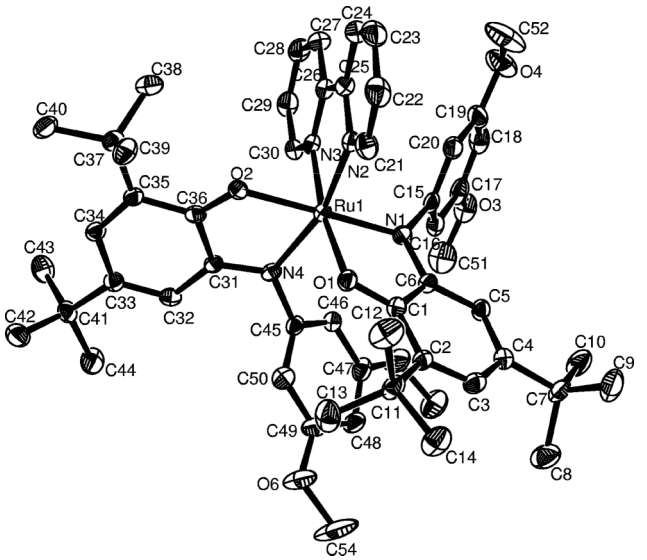

Fig. 9 ORTEP diagram of the cationic part of [**3**](ClO$_4$)$_2$. Ellipsoids are drawn at 50% probability. The counter anions (ClO$_4^-$) and hydrogen atoms are omitted for clarity.

1.355(4) Å, respectively, (Table 2) follow the same trend as has been predicted by DFT for the analogous **2**$^{2+}$ (Tables S14, S15‡). Unlike the ^{1}H NMR spectrum of the **3** the doubly oxidised diamagnetic **3**$^{2+}$ exhibits calculated number of sharp proton resonances (Fig. 10, see the Experimental section).

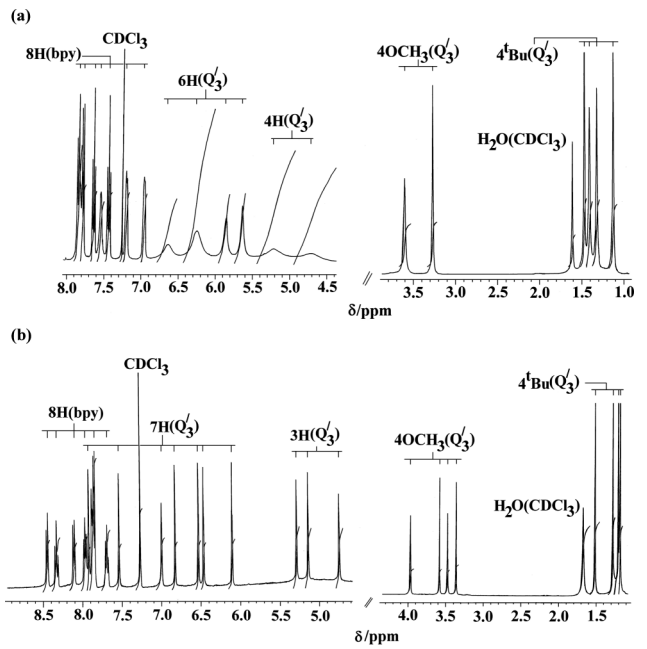

Fig. 10 ^{1}H NMR spectra of (a) **3** and (b) **3**$^{2+}$ in CDCl$_3$.

Commensurate with the quinone dominated LUMO(β-spin) in **2a** and **2b** (~90% Q′, Tables S6a and S7,‡ respectively) the observed reduction in **1–3** (Fig. 7, Table 5) is likely to take place at the Q′ centre. The ~90% Q′ based β-HOMO of the reduced state of **2a**$^-$ or **2b**$^-$ (Tables S12 and S13‡) also justifies the valence formulation of [(bpy)Ru^{II}((Q′$_{Sq}$)(Q′$_{Cat}$)]$^-$ for **1**$^-$–**3**$^-$. The DFT calculated C–O, C–N and C–C (*meta*) bond distances of coordinated Q′ have

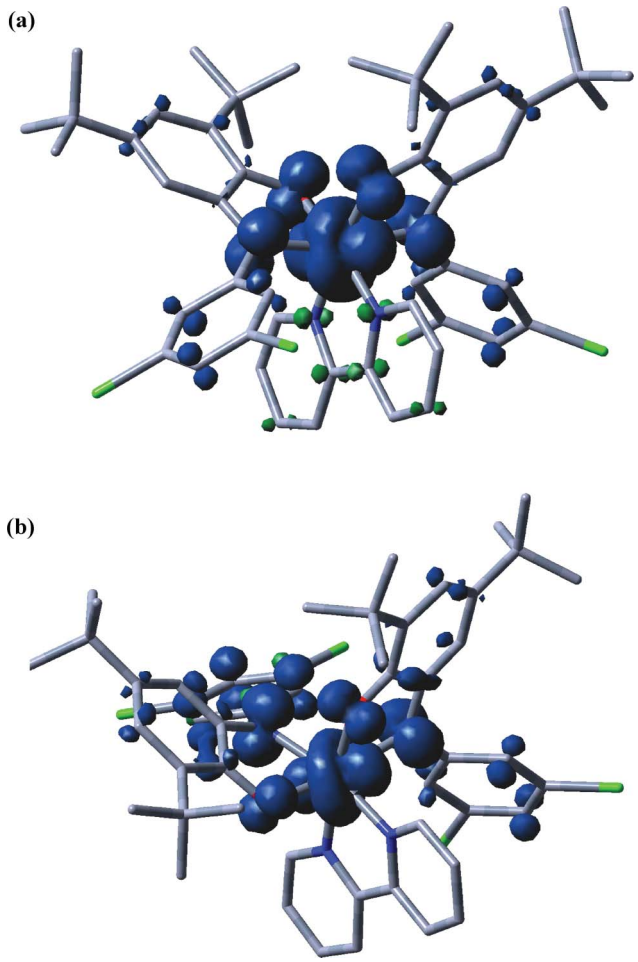

Fig. 11 DFT calculated spin density plots of (a) **2a**$^-$ and (b) **2b**$^-$.

also increased accordingly (Tables S14 and S15‡). The DFT predicted appreciable Mulliken spin density on Ru (~0.4) along with ~0.6 spin density on Q′ in **2a**$^-$ or **2b**$^-$ (Table 3, Fig. 11) however suggests a mixed situation of [(bpy)Ru^{II}(Q′$_{Sq}$)(Q′$_{Cat}$)]$^-$ and [(bpy)Ru^{III}(Q′$_{Cat}$)(Q′$_{Cat}$)]$^-$ (reduction of two Q′$_{Sq}$ centres associated with one-step metal oxidation, Ru^{II} to Ru^{III}, leading to an eventual one-electron reduction).[9i,28] The free radical type EPR spectra with varying metal contributions[9e] for **2a**$^-$ and **2b**$^-$ in CH$_3$CN at 110 K (Fig. S7,‡ **2a**$^-$: g_1, 2.131; g_2, 2.069; g_3, 1.955; <g>; 2.052; Δg, 0.176 and **2b**$^-$: g_1, 2.046; g_2, 2.0007; g_3, 1.989; <g>; 2.014; Δg, 0.057) also reveal the above mentioned mixed situation in **1**$^-$–**3**$^-$.

The electronic spectral features of **1**^{n}–**3**^{n} (n = 0,+1,+2,–1) in CH$_3$CN vary slightly based on the substituents present in the frameworks of Q′ as well as isomeric structural features of **2a** and **2b** (Fig. 12, Table 6). The key transitions in **1**^{n}–**3**^{n} are assigned based on the TD–DFT calculations on the representative **2a**^{n} and **2b**^{n} (Table 7, Tables S16, S17‡). **1–3** exhibit one intense low-energy transition around 950 nm ($\varepsilon \geq 10000$ dm^3 mol^{-1} cm^{-1}) followed by one moderately intense visible transition near 550 nm besides the intra-ligand transitions in the higher energy UV region. The bands near 950 and 550 nm are assigned based on the TD–DFT calculations on **2a** or **2b** as interligand (π)Q′→(π*)bpy and (dπ)Ru,(π)Q′→(π*)bpy MLLCT (MLLCT: metal–ligand to ligand charge-transfer) transitions, respectively.

Table 7 Selected visible energy transitions at the TD–DFT/B3LYP/6-31G(d) level for **2a**^{n}

Complexes	Wavelength(nm) Calcd (oscillator strength, f)	Exp.	Transition	Character
2a	955.4 (0.0214)	950	(63%)SOMO2 → LUMO(α)	(π)Q′$_2$ → (π*)bpy
	566.3 (0.0513)	550	(53%)HOMO-3(α) → LUMO+1(α)	(dπ)Ru/(π)Q′$_2$ → (π*)bpy
			(27%)HOMO-2(β) → LUMO+3(β)	
2a$^+$	934.6 (0.0098)	968	(60%)HOMO-1(β) → LUMO(β)	(dπ)Ru/(π)Q′$_2$ → (π*)Q′$_2$
	671.7(0.2001)	677	(43%)HOMO-3(β) → LUMO(β)	(dπ)Ru/(π)Q′$_2$ → (π*)Q′$_2$
	505.9 (0.0709)	488	(48%)HOMO-2(β) → LUMO+1(β)	(dπ)Ru/(π)Q′$_2$ → (π*)Q′$_2$
			(22%)HOMO-3(β) → LUMO+1(β)	
2a^{2+}	645.6 (0.2040)	660	(84%)HOMO-2 → LUMO	(dπ)Ru/(π)Q′$_2$ → (π*)Q′$_2$
	512.8 (0.1659)	492	(48%)HOMO-2(β) → LUMO+1(β)	(dπ)Ru/(π)Q′$_2$ → (π*)Q′$_2$
			(22%)HOMO-3(β) → LUMO+1(β)	
2a$^-$	967.5 (0.0175)	912	(88%)HOMO-1(β) → LUMO(β)	(dπ)Ru/(π)Q′$_2$ → (π*)bpy
	627.2 (0.0513)	633	(87%)HOMO-4(β) → LUMO+1(β)	(dπ)Ru/(π)Q′$_2$ → (π*)bpy

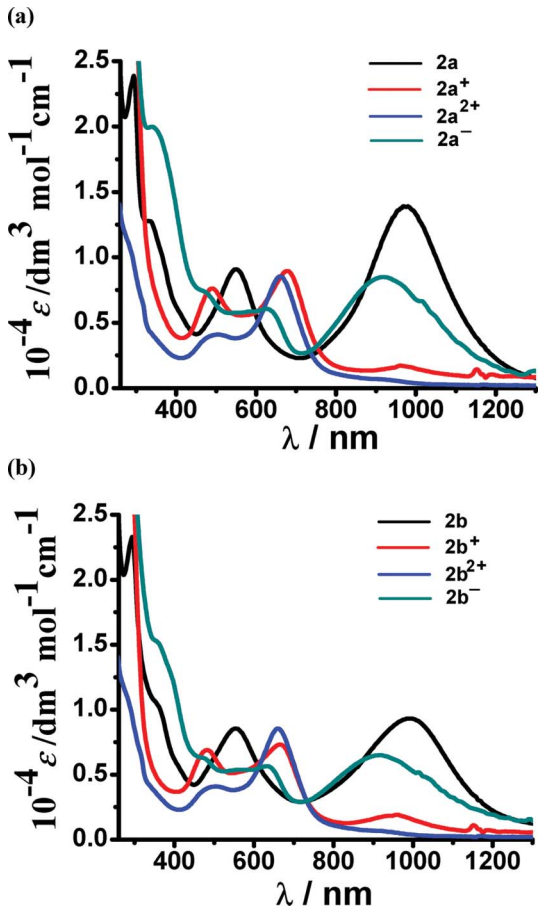

Fig. 12 UV-VIS-NIR spectra in CH_3CN for (a) [**2a**]^n and (b) [**2b**]^n (n = +2: blue, +1: red, 0: black and −1: green).

On one-electron oxidation to [(bpy)Ru^{II}(Q′$_{Sq}$)(Q′$_Q$)]$^+$ (**1**$^+$–**3**$^+$) the intensity of the low-energy transition near 950 nm for the parent **1–3** diminishes drastically from ~15000 to ~2000 dm^3 mol^{-1} cm^{-1}. This can be attributed to the oxidation of one of the Q′$_{Sq}$ centres in **1**$^+$–**3**$^+$. Moreover, **1**$^+$–**3**$^+$ exhibit two new intense visible bands near 670 and 480 nm due to (dπ)Ru,(π)Q′ → (π*)Q′ MLLCT transitions.

The low-energy transition near 950 nm however completely vanishes in case of the doubly oxidised [(bpy)Ru^{II}(Q′$_Q$)$_2$]$^{2+}$ state in **1**$^{2+}$–**3**$^{2+}$ due to the oxidation of both the Q′$_{Sq}$ centres to Q′$_Q$. Two moderately intense visible bands near 650 nm and 500 nm appear for **1**$^{2+}$–**3**$^{2+}$ because of (dπ)Ru,(π)Q′→(π*)Q′ MLLCT transitions.

The reduction of representative **2** to **2**$^-$ pushes the long-wavelength bands to the higher energy region at 912 nm with the reduction in intensity (Tables 6 and 7, Fig. 12). The reduced **2**$^-$ also exhibits two visible region transitions near 630 and 470 nm (Fig. 12, Table 6). The multiple visible region transitions are attributed to MLLCT transitions, (dπ)Ru, (π)Q′ → π*(bpy) involving different HOMOs and LUMOs (Table 7 and Tables S16, S17‡). The DFT predicted low-energy inter-ligand (π)Q′→(π*)bpy transitions in **2**$^-$ (Tables S16, S17‡) in the near-IR region,[9g,29] however, have not been resolved experimentally up to 2000 nm.

Conclusions

Following are the salient features of the present investigation:

- Isomeric ruthenium-bis-iminoquinoid frameworks, [Ru(bpy)-(Q′)$_2$] in **1–3** preferentially stabilise in [(bpy)Ru^{II}(Q′$_{Sq}$)$_2$] valence configuration instead of the alternative valence situation of [(bpy)Ru^{IV}(Q′$_{Cat}$)$_2$] or [(bpy)Ru^{III}(Q′$_{Sq}$)(Q′$_{Cat}$)].

- The spin-state of the complexes having two Q′$_{Sq}$ centres around the Ru(II) ion can be best described as a singlet ground state with a thermally accessible low-lying excited triplet state which results in paramagnetic feature at higher temperatures and diamagnetic behaviour near 2 K.

- The redox-active ruthenium(II) ion and coordinated Q′$_{Sq}$ in **1–3** are likely to participate in electron-transfer processes, however, the coordinated Q′ is preferentially involved in the redox chain: {Ru^{II}(Q′$_Q$)$_2$} ⇌ {Ru^{II}(Q′$_{Sq}$)(Q′$_Q$)} ⇌ {Ru^{II}(Q′$_{Sq}$)$_2$}⇌ {Ru^{II}(Q′$_{Sq}$)(Q′$_{Cat}$)}(major)/{Ru^{III}(Q′$_{Cat}$)(Q′$_{Cat}$)}(minor) leaving the ruthenium(II) ion as a virtual redox-innocent entity.

- The isomeric *ct*-**2a** and *cc*-**2b** exhibit similar valence and spin-state configurations in accessible redox states.

- The unprecedented Ru(II)-iminoquinone derivative, [Ru(bpy)-((Q′$_3$)$_Q$)$_2$](ClO$_4$)$_2$, [**3**](ClO$_4$)$_2$ has been structurally characterised.

The present study with the newer molecular frameworks further demonstrates the sensitivity of the valence and spin situations at the ruthenium–quinonoid interface which indeed introduces vulnerability in establishing the precise electronic structures of such species in accessible redox states. However, the collective understanding of experimental and theoretical events is somewhat effective in reaching to a reasonably conclusive state which also

extends the need for further scrutiny with the more challenging molecular frameworks.

Experimental

Materials

The precursor complex $Ru(bpy)(Cl)_3$[30] and the ligand 2-anilino-4,6-di-*tert*-butylphenol (Q'_{1-3})[6c,31] were prepared according to the reported procedures. Other chemicals and solvents were of reagent grade and used as received.

Physical measurements

UV-VIS-NIR spectra in CH_3CN–0.1 M Et_4NClO_4 at 298 K were recorded on a Perkin-Elmer 950 lambda spectrophotometer. UV-VIS-NIR spectroelectrochemical studies for **2a**$^-$ and **2b**$^-$ were performed in CH_3CN–0.1 M Bu_4NPF_6 at 298 K using an optically transparent thin layer electrode (OTTLE) cell[32] mounted in the sample compartment of a J&M TIDAS spectrophotometer. FT-IR spectra were taken on a Nicolet spectrophotometer with samples prepared as KBr pellets. Solution electrical conductivity was checked using a Systronic 304 conductivity bridge. The EPR measurements were made with a Varian model 109C E-line X-band spectrometer fitted with a quartz dewar for 77 K. The EPR measurements for **2a**$^-$ and **2b**$^-$ were made in a two-electrode capillary tube[33] with a X-band (9.5 GHz) Bruker system ESP300 spectrometer. Cyclic voltammetric, differential pulse voltammetric and coulometric measurements were carried out using a PAR model 273A electrochemistry system. Platinum wire working and auxiliary electrodes and an aqueous saturated calomel reference electrode (SCE) were used in a three-electrode configuration. The supporting electrolyte was 0.1 mol dm^{-3} $[NEt_4]ClO_4$ and the solute concentration was ~10^{-3} mol dm^{-3}. The half-wave potential E°_{298} was set equal to $0.5(E_{pa} + E_{pc})$, where E_{pa} and E_{pc} are the anodic and cathodic cyclic voltammetric peak potentials, respectively. A platinum wire-gauze working electrode was used in the coulometric experiments. The elemental analyses were carried out with a Perkin-Elmer 240C elemental analyzer. Electrospray mass spectra were recorded on a Micromass Q-ToF mass spectrometer. ^{1}H NMR spectra of **1**, **2a**, **2b**, **3**, **3**$^{2+}$ were obtained with 300 MHz Varian and 400 MHz Bruker FT spectrometers, respectively.

Preparation of complexes

The complexes were prepared by following a general procedure. The details are given for one representative complex, **1**.

Synthesis of [Ru(bpy)(Q′$_1$)$_2$] (1). The ligand 2-anilino-4,6-di-*tert*-butylphenol ($H_2Q'_1$) (203 mg, 0.686 mmol) and NaOH (70 mg, 1.75 mmol) were added to a 30 cm^3 ethanolic solution of $Ru(bpy)(Cl)_3$ (100 mg, 0.274 mmol). The mixture was heated to reflux for 16 h under a dinitrogen atmosphere. The initial brown colour changed to red–violet. The solvent of the reaction mixture was evaporated to dryness under reduced pressure. It was then purified on a silica gel column (60–120 mesh). The product corresponding to **1** was eluted with acetonitrile. Evaporation of the solvent under reduced pressure afforded the pure complex.

Yield: 150 mg (65%); Anal. calcd: C, 70.72; H, 6.89; N, 6.60. Found: C, 70.65; H, 6.79; N, 6.36. ESI MS (CH_3CN), *m*/*z* calcd for [**1**]$^+$: 848.36; found: 848.39. ^{1}H NMR ($CDCl_3$), δ (ppm)(*J*/Hz) bpy resonances: 7.76 (2H, d, 7.2), 7.69 (2H, d, 8.4), 7.58 (2H, dd (doublet of doublets), 7.8,7.5), 7.40 (2H, dd, 7.5, 7.5). Q'_1 resonances: 7.55 (2H, broad), 7.18 (3H, broad), 6.87 (4H, broad), 6.67 (1H, broad), 6.38 (2H, broad), 5.67 (2H, broad), 1.39 (9H(^{t}Bu), s), 1.34 (9H(^{t}Bu), s), 1.25 (9H(^{t}Bu), s), 1.12 (9H, s).

Chromatographic separation of isomeric complexes [Ru(bpy)(Q′$_2$)$_2$)] (2a and 2b). Complex **2** was synthesized by following the above mentioned procedure but by using the ligand $H_2Q'_2$ instead of $H_2Q'_1$. This led to the formation of a mixture of two isomers, *ct*-isomeric, **2a** and *cc*-isomeric **2b** which were separated by using a silica gel column (60–120 mesh). The isomer **2b** was eluted initially by dichloromethane and the other isomer **2a** was collected next by using acetonitrile as an eluant. The subsequent evaporation of the solvents under reduced pressure yielded the pure complexes.

2a. Yield: 120 mg (44%); Anal. calcd: C, 60.96; H, 5.53; N, 5.69. Found: C, 60.80; H, 5.51; N, 5.59. ESI MS (CH_3CN), *m*/*z* calcd for [**2a**]$^+$: 985.84; found: 986.30. ^{1}H NMR ($CDCl_3$), δ (ppm) (*J*/Hz), bpy resonances: 7.92 (1H, d, 8.1), 7.64 (1H, dd, 7.5, 7.8), 7.46 (1H, d, 8.0), 7.14 (1H, dd, 5.7, 5.7). Q'_2 resonances: 6.37 (1H, broad), 5.82 (2H, broad), 1.57 (2H, broad), 1.34 (9H(^{t}Bu), s), 1.12 (9H(^{t}Bu), s).

2b. Yield: 70 mg (26%); Anal. calcd: C, 60.96; H, 5.53; N, 5.69. Found: C, 60.70; H, 5.50; N, 5.50. ESI MS (CH_3CN), *m*/*z* calcd for [**2b**]$^+$: 985.84; found: 986.39. ^{1}H NMR ($CDCl_3$) δ (ppm)(*J*/Hz), bpy resonances: 7.86 (1H, dd, 7.2, 7.2), 7.74 (1H, d, 7.6), 7.65 (1H, dd, 8.4, 6.8), 7.48 (1H, d, 4.8), 7.38 (1H, broad), 7.31 (1H, broad), 7.20 (1H, broad), 7.10 (1H, broad). Q'_2 resonances: 6.98 (2H, s), 6.92 (1H, s), 6.82 (1H, s), 6.78 (1H, s), 6.65 (1H, s), 6.54 (2H, s), 6.11 (1H, s), 5.14(1H, s), 1.48 (9H(^{t}Bu), s), 1.29 (9H(^{t}Bu), s), 1.27 (9H(^{t}Bu), s), 1.23 (9H(^{t}Bu), s).

Synthesis of [Ru(bpy)(Q′$_3$)$_2$] (3) and [Ru(bpy)(Q′$_3$)$_2$](ClO$_4$)$_2$ [3](ClO$_4$)$_2$. The complex **3** was prepared by following the same procedure as stated above for the complex **1** but by using the ligand $H_2Q'_3$ instead of $H_2Q'_1$. However, during the chromatographic purification on a silica gel column the complex **3** was partially oxidised to the blue coloured **3**$^{2+}$ state. Thus, **3** and oxidised **3**$^{2+}$ in the form of [**3**]$(ClO_4)_2$ were separately eluted by CH_3CN and a mixture of $HClO_4$ (0.05 cm^3) in CH_3OH (20 cm^3), respectively.

3. Yield: 130 mg (49%); Anal. calcd: C, 66.91; H, 6.87; N, 5.78. Found: C, 66.67; H, 6.76; N, 5.57. ESI MS (CH_3CN), *m*/*z* calcd for [**3**]$^+$: 968.18; found: 968.40. ^{1}H NMR ($CDCl_3$) δ (ppm) (*J*, Hz), bpy resonances: 7.86 (2H, d, 8.0), 7.79 (1H, d, 8.0), 7.64 (1H, dd, 8.0, 7.6), 7.54 (1H, broad), 7.44 (1H, dd, 7.6, 7.6), 7.20 (1H, d, 4.4), 6.97 (1H, broad). Q'_3 resonances: 6.64 (1H, broad), 6.25 (3H, broad), 5.85 (1H, broad), 5.64 (1H, broad), 5.22 (2H, broad), 4.72 (2H, broad), 3.60 (6H(OMe), s), 3.27 (6H(OMe), s), 1.47 (9H(^{t}Bu), s), 1.40 (9H(^{t}Bu), s), 1.32 (9H(^{t}Bu), s), 1.13 (9H(^{t}Bu), s).

[**3**]$(ClO_4)_2$. Yield: 50 mg (16%); Anal. calcd: C, 55.56; H, 5.70; N, 4.80. Found: C, 55.67; H, 5.76; N, 4.57. ESI MS (CH_3CN), *m*/*z* calcd for ([**3**](ClO_4))$^+$: 1067.58; found: 1067.44. ^{1}H NMR ($CDCl_3$) δ (ppm) (*J*, Hz), bpy resonances: 8.45 (1H, d, 8.1), 8.34 (1H, dd, 6.9, 8.0), 8.15 (1H, d, 8.4), 7.96 (1H, dd, 8.0, 8.0), 7.85 (3H, m), 7.70 (1H, dd, 8.0, 6.9). Q'_3 resonances: 7.91 (1H, s), 7.53 (1H, s), 7.00 (1H, s), 6.82 (1H, s), 6.53 (1H, s), 6.47

(1H, s), 6.10 (1H, s), 5.28 (1H, s), 5.13 (1H, s), 4.74 (1H, s), 3.97 (3H(OMe), s), 3.58 (3H(OMe), s), 3.47 (3H(OMe), s), 3.39 (3H(OMe), s), 1.51 (9H(^{t}Bu), s), 1.28 (9H(^{t}Bu), s), 1.20 (9H(^{t}Bu), s), 1.18 (9H(^{t}Bu), s). Electronic spectral data in CH_3CN (λ/nm (ε/dm^3 mol $^{-1}$cm^{-1})): 645(8350), 458(3310). IR data ($\nu(ClO_4^-)$): 1086.36 cm^{-1} and 623.18 cm^{-1}.

X-Ray crystal structure analysis

Single crystals of **1**, **2a**, **2b**, **3** and $\mathbf{3}^{2+}$ were grown by slow evaporation of their acetonitrile solutions at 298 K. X-Ray diffraction data were collected using an OXFORD XCALIBUR-S CCD single crystal X-ray diffractometer. The structures were solved and refined by full-matrix least-squares techniques on F^2 using the SHELX-97 program.[34] The absorption corrections were done by the multi-scan technique. All data were corrected for Lorentz and polarization effects, and the non-hydrogen atoms were refined anisotropically. Hydrogen atoms were included in the refinement process as per the riding model. CCDC nos. for **2a**, **2b**, **3**, and [**3**]$(ClO_4)_2$ are 821453, 821454, 821455, 821456, respectively.

Computational methods

Full geometry optimisations were carried out using the density functional theory method without any symmetry constraints at the (U)B3LYP for **2a**,**2b**,$\mathbf{2a}^+$,$\mathbf{2b}^+$,$\mathbf{2a}^-$,$\mathbf{2b}^-$ and (R)B3LYP level for $\mathbf{2a}^{2+}$, $\mathbf{2b}^{2+}$.[35] All elements except ruthenium were assigned the 6-31G(d) basis set. The SDD basis set with effective core potential was employed for the ruthenium atom.[36] The vibrational frequency calculations were performed to ensure that the optimised geometries represent the local minima and there are only positive eigenvalues. All calculations were performed with Gaussian03 program package.[37] The broken symmetry formalism[38] as implemented in G03 has been applied for **2a**. The broken symmetry formalism using unrestricted B3LYP functional has been proved to be a good approximation for multi-reference ground state involving open shell diradical metal complexes.[6h,20a] The stability of this unrestricted Kohn–Sham solution has been checked by stability analysis as implemented in G03. The BS(m,n)[38c] notation has been adopted in that regard where m(n) denotes the number of spin up (spin down) electrons at the two interacting fragments. The value of S_{ab} has been calculated according to the literature reported procedure.[6h,20a] The energy difference between singlet state and BS(1,1) state is further verified by BMK[38d] and TPSS[38e] levels with same basis set combination. Natural bond orbital analyses were performed using the NBO 3.1 module of Gaussian03.[39] Vertical electronic excitations based on B3LYP optimised geometries were computed for the time-dependent density functional theory (TD–DFT) formalism[40] in acetonitrile using conductor-like polarisable continuum model (CPCM).[41] GaussSum[42] was used to calculate the fractional contributions of various groups to each molecular orbital.

Magnetic measurements

The variable-temperature magnetic susceptibilities were measured on polycrystalline samples with a Quantum Design MPMS*XL* SQUID (Superconducting Quantum Interference Device) susceptometer over a temperature range of 2 to 300 K at constant field of 1 T. Each raw data set was corrected for the diamagnetic contribution of both the sample holder and the complex to the susceptibility. Molar diamagnetic corrections were calculated on the basis of Pascal constants. Magnetization measurements were carried out at 2 and 300 K from 0 to 5 T.

Acknowledgements

Financial support received from the Department of Science and Technology, University Grant commission and Council of Scientific and Industrial Research (New Delhi, India), the Spanish MICINN, CM and UCM-BSCH (projects no. CTQ2008-00920, S-0505-MAT-0303, and UCM-921073-4120824) is gratefully acknowledged. X-Ray structural studies were carried out at the National Single Crystal Diffractometer Facility, Indian Institute Technology Bombay. ^{1}H NMR and EPR experiments were carried out at the Sophisticated Analytical Instrument Facility (SAIF), Indian Institute of Technology Bombay.

References

1 (*a*) H. Nohl, W. Jordan and R. I. Youngman, *Adv. Free Radical Biol. Med.*, 1986, **2**, 211; (*b*) S. D. Thomson, *Naturally Occurring Quinones IV*, Springer, The Netherlands, 1996; (*c*) J. L. Bolton, M. A. Trush, T. M. Penning, G. Dryhurst and T. J. Monks, *Chem. Res. Toxicol.*, 2000, **13**, 135.

2 (*a*) J. A. Duine and J. A. Jongejan, in *Bioinorganic Catalysis*, ed. J. Reedijk, Marcel Dekker, New York, 1993, p. 447; (*b*) J. P. Klinman, *Proc. Natl. Acad. Sci. U. S. A.*, 2001, **98**, 705; (*c*) M. Mure, S. A. Mills and J. P. Klinman, *Biochemistry*, 2002, **41**, 9269; (*d*) S. X. Wang, N. Nakamura, M. Murell, J. P. Klinman and J. Sanders-Loehr, *J. Biol. Chem.*, 1997, **272**, 28841; (*e*) M. Mure, S. X. Wang and J. P. Klinman, *J. Am. Chem. Soc.*, 2003, **125**, 6113; (*f*) C. Anthony, *Arch. Biochem. Biophys.*, 2004, **428**, 2; (*g*) C. Anthony, *Biochem. J.*, 1996, **320**, 697.

3 Y. Izumi, H. Sawada, N. Sakka, N. Yamamoto, T. Kume, H. Katsuki, S. Shimohama and A. Akaike, *J. Neurosci. Res.*, 2005, **79**, 849.

4 (*a*) B. Furie, B. A. Bouchard and B. C. Furie, *Blood*, 1999, **93**, 1798; (*b*) R. Meganathan, *Vitam. Horm.*, 2001, **61**, 173; (*c*) M. He, P. J. Sheldon and D. H. Sherman, *Proc. Natl. Acad. Sci. U. S. A.*, 2001, **98**, 926.

5 (*a*) P. Zanello and M. Corsini, *Coord. Chem. Rev.*, 2006, **250**, 2000; (*b*) K. P. Butin, E. K. Beloglazkina and N. V. Zyk, *Russ. Chem. Rev.*, 2005, **74**, 531; (*c*) C. G. Pierpont, *Coord. Chem. Rev.*, 2001, **219–221**, 415; (*d*) C. G. Pierpont and C. W. Lange, *Prog. Inorg. Chem.*, 1994, **41**, 331; (*e*) A. Vlček Jr., *Comments Inorg. Chem.*, 1994, **16**, 207; (*f*) W. Kaim, *Coord. Chem. Rev.*, 1987, **76**, 187; (*g*) C. G. Pierpont and R. M. Buchanan, *Coord. Chem. Rev.*, 1981, **38**, 45; (*h*) S. Roy, B. Sarkar, D. Bubrin, M. Niemeyer, S. Zalis, G. K. Lahiri and W. Kaim, *J. Am. Chem. Soc.*, 2008, **130**, 15230; (*i*) A. M. Morris, C. G. Pierpont and R. G. Finke, *Inorg. Chem.*, 2009, **48**, 3496; (*j*) Y. Suenaga and C. G. Pierpont, *Inorg. Chem.*, 2005, **44**, 6183; (*k*) C. M. Liu, E. Nordlander, D. Schmeh, R. Shoemaker and C. G. Pierpont, *Inorg. Chem.*, 2004, **43**, 2114; (*l*) M. D. Ward and J. A. McCleverty, *J. Chem. Soc., Dalton Trans.*, 2002, 275; (*m*) W. Kaim and B. Schwederski,, *Coord. Chem. Rev.*, 2010, **254**, 1580; (*n*) C. G. Pierpont and A. S. Attia, *Collect. Czech. Chem. Commun.*, 2001, **66**, 33; (*o*) A. Y. Girgis, Y. S. Sohn and A. L. Balch, *Inorg. Chem.*, 1975, **14**, 2327; (*p*) B. Schwederski, V. Kasack, W. Kaim, E. Roth and J. Jordanov, *Angew. Chem., Int. Ed. Engl.*, 1990, **29**, 78; (*q*) S. Frantz, J. Rall, I. Hartenbach, T. Schleid, S. Zalis and W. Kaim, *Chem.–Eur. J.*, 2004, **10**, 149; (*r*) C. Mukherjee, T. Weyhermüller, E. Bothe and P. Chaudhuri, *Inorg. Chem.*, 2008, **47**, 2740; (*s*) O. Siri and P. Braunstein, *Chem. Commun.*, 2000, 2223; (*t*) M. Elhabiri, O. Siri, A. Sornosa-Tent, A.-M. Albrecht-Gary and P. Braunstein, *Chem.–Eur. J.*, 2004, **10**, 134; (*u*) P. Braunstein, A. Demessence, O. Siri and J.-P. Taquet, *C. R. Chim.*, 2004, **7**, 909; (*v*) O. Siri, P. Braunstein, M. M. Rohmer, M. Bénard and R. Welter, *J. Am. Chem. Soc.*, 2003, **125**, 13793; (*w*) A. Paretzki, R. Pattacini, R. Huebner, P. Braunstein and B. Sarkar, *Chem. Commun.*, 2010, **46**, 1497.

6 (*a*) D. Herebian, E. Bothe, E. Bill, T. Weyhermüller and K. Wieghardt, *J. Am. Chem. Soc.*, 2001, **123**, 10012; (*b*) C. N. Verani, S. Gallert, E. Bill, T. Weyhermüller, K. Wieghardt and P. Chaudhuri, *Chem.*

Commun., 1999, 1747; (*c*) P. Chaudhuri, C. N. Verani, E. Bill, E. Bothe, T. Weyhermüller and K. Wieghardt, *J. Am. Chem. Soc.*, 2001, **123**, 2213; (*d*) H. Chun, E. Bill, E. Bothe, T. Weyhermüller and K. Wieghardt, *Inorg. Chem.*, 2002, **41**, 5091; (*e*) P. Ghosh, A. Begum, D. Herebian, E. Bothe, K. Hildenbrand, T. Weyhermüller and K. Wieghardt, *Angew. Chem., Int. Ed.*, 2003, **42**, 563; (*f*) K. S. Min, T. Weyhermüller and K. Wieghardt, *Dalton Trans.*, 2003, 1126; (*g*) K. Ray, A. Begum, T. Weyhermüller, S. Piligkos, J. v. Slageren, F. Neese and K. Wieghardt, *J. Am. Chem. Soc.*, 2005, **127**, 4403; (*h*) V. Bachler, G. Olbrich, F. Neese and K. Wieghardt, *Inorg. Chem.*, 2002, **41**, 4179; (*i*) A. C. Bowman, C. Milsmann, E. Bill, E. Lobkovsky, T. Weyhermüller, K. Wieghardt and P. J. Chirik, *Inorg. Chem.*, 2010, **49**, 6110; (*j*) S. Sproules, T. Weyhermüller, S. De Beer and K. Wieghardt, *Inorg. Chem.*, 2010, **49**, 5241; (*k*) S. Sproules, F. L. Benedito, E. Bill, T. Weyhermüller, S. DeBeer George and K. Wieghardt, *Inorg. Chem.*, 2009, **48**, 10926; (*l*) C. C. Lu, T. Weyhermüller, E. Bill and K. Wieghardt, *Inorg. Chem.*, 2009, **48**, 6055; (*m*) N. Roy, S. Sproules, T. Weyhermüller and K. Wieghardt, *Inorg. Chem.*, 2009, **48**, 3783; (*n*) N. Roy, S. Sproules, E. Bill, T. Weyhermüller and K. Wieghardt, *Inorg. Chem.*, 2008, **47**, 10911; (*o*) K. Ray, S. DeBeer George, E. I. Solomon, K. Wieghardt and F. Neese, *Chem.–Eur. J.*, 2007, **13**, 2783; (*p*) A. Mondal, T. Weyhermüller and K. Wieghardt, *Chem. Commun.*, 2009, 6098; (*q*) A. C. Bowman, C. Milsmann, A. Hojilla, C. Crisita, E. Lobkovsky, K. Wieghardt and P. J. Chirik, *J. Am. Chem. Soc.*, 2010, **132**, 1676; (*r*) C. Milsmann, S. Sproules, E. Bill, T. Weyhermüller, S. D. George and K. Wieghardt, *Chem.–Eur. J.*, 2010, **16**, 3628.

7 (*a*) H. Masui, A. L. Freda, M. C. Zerner and A. B. P. Lever, *Inorg. Chem.*, 2000, **39**, 141; (*b*) A. B. P. Lever, H. Masui, R. A. Metcalfe, D. J. Stufkens, E. S. Dodsworth and P. R. Auburn, *Coord. Chem. Rev.*, 1993, **125**, 317; (*c*) S. I. Gorelsky, A. B. P. Lever and M. Ebadi, *Coord. Chem. Rev.*, 2002, **230**, 97; (*d*) A. B. P. Lever, *Coord. Chem. Rev.*, 2010, **254**, 1397; (*e*) A. B. P. Lever and S. I. Gorelsky, *Coord. Chem. Rev.*, 2000, **208**, 153; (*f*) S. I. Gorelsky, E. S. Dodsworth, A. B. P. Lever and A. A. Vlcek, *Coord. Chem. Rev.*, 1998, **174**, 469; (*g*) S. D. J. McKinnon, B. O. Patrick, A. B. P. Lever and R. G. Hicks, *Chem. Commun.*, 2010, **46**, 773; (*h*) R. A. Begum, A. A. Farah, H. N. Hunter and A. B. P. Lever, *Inorg. Chem.*, 2009, **48**, 2018; (*i*) D. Kalinina, D. Dares, H. Kaluarachchi, P. G. Potvin and A. B. P. Lever, *Inorg. Chem.*, 2008, **47**, 10110; (*j*) A. P. Meacham, K. L. Druce, Z. R. Bell, M. D. Ward, J. B. Keister and A. B. P. Lever, *Inorg. Chem.*, 2003, **42**, 7887; (*k*) A. B. P. Lever and S. L. Gorelsky, *Struct. Bonding (Berlin)*, 2004, **107**, 77; (*l*) H. Masui, A. B. P. Lever and P. Auburn, *Inorg. Chem.*, 1991, **30**, 2402; (*m*) M. Haga, E. S. Dodsworth and A. B. P. Lever, *Inorg. Chem.*, 1986, **25**, 447; (*n*) M. Ebadi and A. B. P. Lever, *Inorg. Chem.*, 1999, **38**, 467; (*o*) P. R. Auburn, E. S. Dodsworth, M. Haga, W. Liu, W. A. Nevin and A. B. P. Lever, *Inorg. Chem.*, 1991, **30**, 3502; (*p*) M. Haga, E. S. Dodsworth, A. B. P. Lever, S. R. Boone and C. G. Pierpont, *J. Am. Chem. Soc.*, 1986, **108**, 7413; (*q*) A. DelMedico, E. S. Dodsworth, A. B. P. Lever and W. J. Pietro, *Inorg. Chem.*, 2004, **43**, 2654; (*r*) C. J. da Cunha, E. S. Dodsworth, M. A. Monteiro and A. B. P. Lever, *Inorg. Chem.*, 1999, **38**, 5399; (*s*) R. Santana da Silva, S. I. Gorelsky, E. S. Dodsworth, E. Tfouni and A. B. P. Lever, *J. Chem. Soc., Dalton Trans.*, 2000, 4078; (*t*) J. Rusanova, E. Rusanov, S. I. Gorelsky, D. Christendat, R. Popescu, A. A. Farah, R. Beaulac, C. Reber and A. B. P. Lever, *Inorg. Chem.*, 2006, **45**, 6246; (*u*) R. A. Metcalfe and A. B. P. Lever, *Inorg. Chem.*, 1997, **36**, 4762; (*v*) H. Masui, A. B. P. Lever and E. S. Dodsworth, *Inorg. Chem.*, 1993, **32**, 258; (*w*) R. Beaulac, A. B. P. Lever and C. Reber, *Eur. J. Inorg. Chem.*, 2007, 48; (*x*) S. I. Gorelsky and A. B. P. Lever, *Can. J. Anal. Sci. Spectrosc.*, 2003, **48**, 93.

8 (*a*) J. L. Boyer, J. Rochford, M. K. Tsai, J. T. Muckerman and E. Fujita, *Coord. Chem. Rev.*, 2010, **254**, 309; (*b*) M. D. Ward, *Inorg. Chem.*, 1996, **35**, 1712; (*c*) M. Kurihara, S. Daniele, K. Tsuge, H. Sugimoto and K. Tanaka, *Bull. Chem. Soc. Jpn.*, 1998, **71**, 867; (*d*) R. Okamura, T. Wada, K. Aikawa, T. Nagata and K. Tanaka, *Inorg. Chem.*, 2004, **43**, 7210; (*e*) K. Kobayashi, H. Ohtsu, T. Wada, T. Kato and K. Tanaka, *J. Am. Chem. Soc.*, 2003, **125**, 6729; (*f*) K. N. Mitra, S. Choudhury, A. Castiñeiras and S. Goswami, *J. Chem. Soc., Dalton Trans.*, 1998, 2901; (*g*) M. K. Milcic, B. D. Ostojic and S. D. Zaric, *Inorg. Chem.*, 2007, **46**, 7109; (*h*) R. B. Salmonsen, A. Abelleira, M. J. Clarke and S. D. Pell, *Inorg. Chem.*, 1984, **23**, 385; (*i*) R. O. Rosete, D. J. Cole-Hamilton and G. Wilkinson, *J. Chem. Soc., Dalton Trans.*, 1979, 1618; (*j*) H. S. Das, F. Weisser, D. Schweinfurth, C.-Y. Su, L. Bogani, J. Fiedler and B. Sarkar, *Chem.–Eur. J.*, 2010, **16**, 2977; (*k*) K. N. Mitra, P. Majumdar, S. M. Peng, A. Castiñeiras and S. Goswami, *Chem. Commun.*, 1997, 1267; (*l*) C. Das, K. K. Kamar, A. K. Ghosh, P. Majumdar, C.-H. Hung and S. Goswami, *New J. Chem.*, 2002, **26**, 1409; (*m*) A. Dei, D. Gatteschi and L. Pardi, *Inorg. Chem.*, 1990, **29**, 1442; (*n*) A. M. Barthram, R. L. Cleary, R. Kowallick and M. D. Ward, *Chem. Commun.*, 1998, 2695; (*o*) S. Ye, B. Sarkar, C. Duboc, J. Fiedler and W. Kaim, *Inorg. Chem.*, 2005, **44**, 2843; (*p*) E. Waldhör, B. Schwederski and W. Kaim, *J. Chem. Soc., Perkin Trans. 2*, 1993, 2109; (*q*) S. Ernst, P. Hänel, J. Jordanov, W. Kaim, V. Kasack and E. Roth, *J. Am. Chem. Soc.*, 1989, **111**, 1733; (*r*) S. Ernst, V. Kasack, C. Bessenbacher and W. Kaim, *Z. Naturforsch.*, 1987, **42b**, 425; (*s*) V. Kasack, W. Kaim, H. Binder, J. Jordanov and E. Roth, *Inorg. Chem.*, 1995, **34**, 1924; (*t*) A. Knödler, J. Fiedler and W. Kaim, *Polyhedron*, 2004, **23**, 701; (*u*) S. Chatterjee, P. Singh, J. Fiedler, R. Bakova, S. Zalis, W. Kaim and S. Goswami, *Dalton Trans.*, 2009, 7778; (*v*) S. Samanta, P. Singh, J. Fiedler, S. Zalis, W. Kaim and S. Goswami, *Inorg. Chem.*, 2008, **47**, 1625; (*w*) J. Maurer, M. Linseis, B. Sarkar, B. Schwederski, M. Niemeyer, W. Kaim, S. Zalis, C. Anson, M. Zabel and R. F. Winter, *J. Am. Chem. Soc.*, 2008, **130**, 259; (*x*) B. Sarkar, S. Frantz, W. Kaim and C. Duboc, *Dalton Trans.*, 2004, 3727.

9 (*a*) C. Remenyi and M. Kaupp, *J. Am. Chem. Soc.*, 2005, **127**, 11399; (*b*) S. Maji, S. Patra, S. Chakraborty, S. M. Mobin, D. Janardanan, R. B. Sunoj and G. K. Lahiri, *Eur. J. Inorg. Chem.*, 2007, 314; (*c*) S. Patra, B. Sarkar, S. M. Mobin,W. Kaim and G. K. Lahiri, *Inorg. Chem.*, 2003, **42**, 6469; (*d*) S. Maji, B. Sarkar, S. M. Mobin, J. Fiedler, F. A. Urbanos, R. Jimenez-Aparicio, W. Kaim and G. K. Lahiri, *Inorg. Chem.*, 2008, **47**, 5204; (*e*) S. Ghumaan, B. Sarkar, S. Maji, V. G. Puranik, J. Fiedler, F. A. Urbanos, R. Jimenez-Aparicio, W. Kaim and G. K. Lahiri, *Chem.–Eur. J.*, 2008, **14**, 10816; (*f*) S. Kar, B. Sarkar, S. Ghumaan, D. Roy, F. A. Urbanos, J. Fiedler, R. B. Sunoj, R. Jimenez-Aparicio, W. Kaim and G. K. Lahiri, *Inorg. Chem.*, 2005, **44**, 8715; (*g*) D. Das, T. K. Mondal, S. M. Mobin and G. K. Lahiri, *Inorg. Chem.*, 2009, **48**, 9800; (*h*) S. Kar, B. Sarkar, S. Ghumaan, D. Janardanan, J. van Slageren, J. Fiedler, V. G. Puranik, R. B. Sunoj, W. Kaim and G. K. Lahiri, *Chem.–Eur. J.*, 2005, **11**, 4901; (*i*) S. Ghumaan, B. Sarkar, S. Patra, J. Van Slageren, J. Fiedler, W. Kaim and G. K. Lahiri, *Inorg. Chem.*, 2005, **44**, 3210; (*j*) D Kumbhakar, B. Sarkar, S. Maji, S. M. Mobin, J. Fiedler, F. A. Urbanos, R. Jimenez-Aparicio, W. Kaim and G. K. Lahiri, *J. Am. Chem. Soc.*, 2008, **130**, 17575; (*k*) A. K. Das, B. Sarkar, C. Duboc, S. Strobel, J. Fiedler, S. Zalis, G. K. Lahiri and W. Kaim, *Angew. Chem., Int. Ed.*, 2009, **48**, 4242; (*l*) A. K. Das, B. Sarkar, J. Fiedler, S. Zalis, I. Hartenbach, S. Strobel, G. K. Lahiri and W. Kaim, *J. Am. Chem. Soc.*, 2009, **131**, 8895; (*m*) D. Kumbhakar, B. Sarkar, A. Das, A. K. Das, S. M. Mobin, J. Fiedler, W. Kaim and G. K. Lahiri, *Dalton Trans.*, 2009, 9645; (*n*) N. Bag, A. Pramanik, G. K. Lahiri and A. Chakravorty, *Inorg. Chem.*, 1992, **31**, 40; (*o*) J. Rochford, M. K. Tsai, D. J. Szalda, J. L. Boyer, J. T. Muckerman and E. Fujita, *Inorg. Chem.*, 2010, **49**, 860; (*p*) S. Maji, B. Sarkar, S. M. Mobin, J. Fiedler, W. Kaim and G. K. Lahiri, *Dalton Trans.*, 2007, 2411; (*q*) S. Patra, B. Sarkar, S. Maji, J. Fiedler, F. A. Urbanos, R. Jimenez-Aparicio, W. Kaim and G. K. Lahiri, *Chem.–Eur. J.*, 2006, **12**, 489; (*r*) S. Ghumaan, S. Mukherjee, S. Kar, D. Roy, S. M. Mobin, R. B. Sunoj and G. K. Lahiri, *Eur. J. Inorg. Chem.*, 2006, 4426.

10 (*a*) J. T. Muckerman, D. E. Polyansky, T. Wada, K. Tanaka and E. Fujita, *Inorg. Chem.*, 2008, **47**, 1787; (*b*) T. Wada, K. Tsuge and K. Tanaka, *Inorg. Chem.*, 2001, **40**, 329; (*c*) T. Wada, K. Tsuge and K. Tanaka, *Angew. Chem., Int. Ed.*, 2000, **39**, 1479; (*d*) M. K. Tsai, J. Rochford, D. E. Polyansky, T. Wada, K. Tanaka, E. Fujita and T. J. Muckerman, *Inorg. Chem.*, 2009, **48**, 4372.

11 G. K. Lahiri and W. Kaim, *Dalton Trans.*, 2010, **39**, 4471.

12 (*a*) W. P. Griffith, C. A. Pumphrey and T. A. Rainey, *J. Chem. Soc., Dalton Trans.*, 1986, 1125; (*b*) S. Bhattacharya, S. R. Boone, G. A. Fox and C. G. Pierpont, *J. Am. Chem. Soc.*, 1990, **112**, 1088; (*c*) D. Das, A. K. Das, B. Sarkar, T. K. Mondal, S. M. Mobin, J. Fiedler, S. Zalis, F. A. Urbanos, R. Jimenez-Aparicio, W. Kaim and G. K. Lahiri, *Inorg. Chem.*, 2009, **48**, 11853.

13 (*a*) A. B. P. Lever, P. R. Auburn, E. S. Dodsworth, M. Haga, W. Liu, M. Melnik and W. A. Nevin, *J. Am. Chem. Soc.*, 1988, **110**, 8076; (*b*) S. R. Boone and C. G. Pierpont, *Inorg. Chem.*, 1987, **26**, 1769; (*c*) N. Bag, G. K. Lahiri, P. Basu and A. Chakravorty, *J. Chem. Soc., Dalton Trans.*, 1992, 113; (*d*) S. Bhattacharya and C. G. Pierpont, *Inorg. Chem.*, 1991, **30**, 1511; (*e*) S. Bhattacharya and C. G. Pierpont, *Inorg. Chem.*, 1994, **33**, 6038; (*f*) P. Belser, A. V. Zelewsky and M. Zehnder, *Inorg. Chem.*, 1981, **20**, 3098.

14 S. Bhattacharya, P. Gupta, F. Basuli and C. G. Pierpont, *Inorg. Chem.*, 2002, **41**, 5810.

15 A. I. Poddel'sky, V. K. Cherkasov and G. A. Abakumov, *Coord. Chem. Rev.*, 2009, **253**, 291.

16 H. Agarwala, D. Das, S. M. Mobin, T. K. Mondal and G. K. Lahiri, *Inorg. Chim. Acta*, 2011, DOI: 10.1016/j.ica.2011.02.079.
17 F. A. Cotton, S. Herrero, R. Jiménez-Aparicio, C. A. Murillo, F. A. Urbanos, D. Villagrán and X. Wang, *J. Am. Chem. Soc.*, 2007, **129**, 12666.
18 R. Podgajny, R. Pezka, C. Desplanches, L. Ducasse, W. Nitek, T. Korzeniak, O. Stefańczyk, M. Rams, B. Sieklucka and M. Verdaguer, *Inorg. Chem.*, 2011, **50**, 3213.
19 (*a*) A. Ozarowski, B. R. McGarvey, C. Peppe and D. G. Tuck, *J. Am. Chem. Soc.*, 1991, **113**, 3288; (*b*) N. S. Hosmane, Y. Wang, H. Zhang, K-J. Lu, J. A. Maguire, T. G. Gray, K. A. Brooks, E. Waldhor, W. Kaim and R. K. Kremer, *Organometallics*, 1997, **16**, 1365; (*c*) N. M. Atherton, *Electron Spin Resonance*, Ellis Horwood, Ltd., Sussex, England, 1973.
20 (*a*) D. Herebian, K. E. Wieghardt and F. Neese, *J. Am. Chem. Soc.*, 2003, **125**, 10997; (*b*) F. Neese, *J. Phys. Chem. Solids*, 2004, **65**, 781; (*c*) I. A. Gass, C. J. Gartshore, D. W. Lupton, B. Moubaraki, A. Nafady, A. M. Bond, J. F. Boas, J. D. Cashion, C. Milsmann, K. Wieghardt and K. S. Murray, *Inorg. Chem.*, 2011, **50**, 3052; (*d*) V. Bachler, P. Chaudhuri and K. Wieghardt, *Chem.–Eur. J.*, 2001, **7**, 404.
21 R. Bauernschmitt and R. Ahlrichs, *J. Chem. Phys.*, 1996, **104**, 9047.
22 B. L. Guennic, T. Floyd, B. R. Galan, J. Autschbach and J. B. Keister, *Inorg. Chem.*, 2009, **48**, 5504.
23 T. Kundu, S. M. Mobin and G. K. Lahiri, *Dalton Trans.*, 2010, **39**, 4232.
24 (*a*) S. S. Kulkarni, B. K. Santra, P. Munshi and G. K. Lahiri, *Polyhedron*, 1998, **17**, 4365; (*b*) S. Kar, B. Sarkar, S. Ghumaan, M. Leboschka, J. Fiedler,W. Kaim and G. K. Lahiri, *Dalton Trans.*, 2007, 1934.
25 B. K. Santra and G. K. Lahiri, *J. Chem. Soc., Dalton Trans.*, 1997, 129.
26 C. Creutz, *Prog. Inorg. Chem.*, 1983, **30**, 1.
27 S. Bhattacharya, *Polyhedron*, 1994, **13**, 451.
28 S. Maji, B. Sarkar, S. Patra, J. Fiedler, S. M. Mobin, V. G. Puranik, W. Kaim and G. K. Lahiri, *Inorg. Chem.*, 2006, **45**, 1316.
29 (*a*) S. Chakraborty, R. H. Laye, R. L. Paul, R. G. Gonnade, V. G. Puranik, M. D. Ward and G. K. Lahiri, *J. Chem. Soc., Dalton Trans.*, 2002, 1172; (*b*) S. Patra, B. Sarkar, S. Ghumaan, J. Fiedler, W. Kaim and G. K. Lahiri, *Dalton Trans.*, 2004, 754.
30 S. Anderson and K. R. Seddon, *J. Chem. Res. (S)*., 1979, 74.
31 S. Mukherjee, T. Weyhermüller, E. Bothe, K. Wieghardt and P. Chaudhuri, *Dalton Trans.*, 2004, 3842.
32 M. Krejcik, M. Danek and F. Hartl, *J. Electroanal. Chem.*, 1991, **317**, 179.
33 W. Kaim, S. Ernst and V. Kasack, *J. Am. Chem. Soc.*, 1990, **112**, 173.
34 G. M. Sheldrick, *SHELX-97, Program for Crystal Structure Solution and Refinement*, University of Göttingen, Germany, 1997.
35 C. Lee, W. Yang and R. G. Parr, *Phys. Rev. B*, 1988, **37**, 785.
36 (*a*) D. Andrae, U. Haeussermann, M. Dolg, H. Stoll and H. Preuss, *Theor. Chim. Acta*, 1990, **77**, 123; (*b*) P. Fuentealba, H. Preuss, H. Stoll and L. V. Szentpaly, *Chem. Phys. Lett.*, 1982, **89**, 418.
37 M. J. Frisch, *et al. Gaussian 03*, Gaussian, Inc., Wallingford CT, 2004.
38 (*a*) A. P. Ginsberg, *J. Am. Chem. Soc.*, 1980, **102**, 111; (*b*) L. Noodleman, C. Y. Peng, D. A. Case and J.-M. Mouesca, *Coord. Chem. Rev.*, 1995, **144**, 199; (*c*) B. Kirchner, F. Wennmohs, S. Ye and F. Neese, *Curr. Opin. Chem. Biol.*, 2007, **11**, 134; (*d*) A. D. Boese and J. M. L. Martin, *J. Chem. Phys.*, 2004, **121**, 3405; (*e*) J. M. Tao, J. P. Perdew, V. N. Staroverov and G. E. Scuseria, *Phys. Rev. Lett.*, 2003, **91**, 146401.
39 E. D. Glendening, A. E. Reed, J. E. Carpenter, F. Weinhold, NBO, version 3.1.
40 (*a*) R. Bauernschmitt and R. Ahlrichs, *Chem. Phys. Lett.*, 1996, **256**, 454; (*b*) R. E. Stratmann, G. E. Scuseria and M. J. Frisch, *J. Chem. Phys.*, 1998, **109**, 8218; (*c*) M. E. Casida, C. Jamorski, K. C. Casida and D. R. Salahub, *J. Chem. Phys.*, 1998, **108**, 4439.
41 (*a*) V. Barone and M. J. Cossi, *J. Phys. Chem. A*, 1998, **102**, 1995; (*b*) M. Cossi and V. Barone, *J. Chem. Phys.*, 2001, **115**, 4708; (*c*) M. Cossi, N. Rega, G. Scalmani and V. Barone, *J. Comput. Chem.*, 2003, **24**, 669.
42 N. M. O'Boyle, A. L. Tenderholt and K. M. Langner, *J. Comput. Chem.*, 2008, **29**, 839.

